Organic & Biomolecular Chemistry

ROYAL SOCIETY OF CHEMISTRY

REVIEW

View Article Online
View Journal | View Issue

Cite this: *Org. Biomol. Chem.*, 2025, **23**, 4593

Fluorohydrins and where to find them: recent asymmetric syntheses of β-fluoro alcohols and their derivatives

Kelly Burchell-Reyes and Jean-François Paquin *

Received 24th February 2025,
Accepted 9th April 2025

DOI: 10.1039/d5ob00330j

rsc.li/obc

Fluorohydrins – or β-fluorinated alcohols – and their fluorinated group derivatives are a biologically relevant class of compounds, with applications ranging from PET tracers to cancer therapeutics. Recent efforts have unlocked asymmetric access to these related motifs through reactions of carbonyls, alkenes, organoboranes, and epoxides or transformations such as cyclizations or ring expansions. The present work provides an overview of synthetic approaches to various fluorohydrins that have been explored in the past decade, as well as selected examples of these syntheses applied to medicinal chemistry.

1 Introduction

Approximately 20% of commercial pharmaceuticals are fluoropharmaceuticals.[1] This is likely due to fluorine's unique properties, enabling it to function as a bioisosteric replacement for a variety of other atoms. As the atom with the second-smallest atomic radius, fluorine can serve as a biosisosteric replacement to hydrogen. Yet, fluorine is highly electronegative and forms the strongest single bond to carbon. A palette of fluorinated groups (Table 1) has been demonstrated to complement fluorine substituents and serve as bioisosteric replacements in different contexts.[2] By careful curation of a fluorinated group's lipophilicity, one might modulate the drug resorption and delivery, while its electronic properties might influence the binding interactions and pK_a of nearby functional groups.[3]

Over 50% of commercial pharmaceuticals are chiral compounds, of which, in a database of the 340 fluoropharmaceuticals approved between 1954–2019, 62 drugs (18%) contained a fluorine or fluorinated group directly connected to a stereocenter (including racemates).[1] Most prevalent were fluorocorticoids (46 drugs) and fluoronucleosides (4 drugs). This scarcity is likely a result of the paucity of existing methods to access these motifs.

PROTEO, CCVC, Département de chimie, Université Laval, Québec, QC, G1V 0A6, Canada. E-mail: jean-francois.paquin@chm.ulaval.ca

Kelly Burchell-Reyes

Kelly Burchell-Reyes completed her Honours BSc Chemistry Co-Op at Concordia University in Montreal, QC, where she garnered multidisciplinary research experiences. She began her doctoral studies at Université Laval in Quebec City under the supervision of Prof. Jean-François Paquin in 2022, with funding from NSERC PGS-D and FRQ-NT Doctoral scholarships. Her research pertains to enantioselective transformations of prochiral fluorinated ketones. She is a member of Empowering Women in Organic Chemistry, Eastern Canada Chapter, and has shared stories of graduate student experiences with University Affairs.

Jean-François Paquin

Jean-François Paquin received his PhD in 2004 from the University of Toronto under the supervision of Prof. Mark Lautens. After a postdoctoral stay in Prof. Erick M. Carreira's lab at the ETH Zürich, he was appointed assistant professor in 2005 at the Université Laval in Quebec City. He was promoted to associate professor in 2010 to full professor in 2014. His research interests include the development of novel methodologies for the synthesis of organofluorine compounds and their applications for the preparation of bioactive fluorinated compounds or fluorinated biological probes. In 2016, he was awarded the Keith Fagnou Award from the Canadian Society for Chemistry.

Table 1 Selected properties of fluorinated groups

	F	CF_3	OCF_3	SCF_3
Pauling electronegativity (χ_r)	3.98[4]	3.46[5]	3.74[5]	—
Meta substituent constant (σ_m)	0.337[6]	0.43[7]	0.38[8]	0.40[9]
Para substituent constant (σ_p)	0.062[7]	0.54[7]	0.35[9]	0.50[9]
Hydrophobicity (π)	0.14[10]	0.88[10]	1.04[10]	1.44[10]

Fluorohydrins and their derivatives are a well-established motif in medicinal chemistry, with applications in treatments such as Sofosbuvir and Dexamethosone and PET tracers including [^{18}F]MISO and [^{18}F]THK-5351 (Fig. 1). As increasingly complex fluorinated groups are developed, new synthetic methods to form derivatives of established bioactive motifs are required.

Recent advances towards the enantioselective formation of β-CF_3, β-OCF_3, and β-SCF_3 alcohols have gained traction. Synthetic strategies and approaches show some overlap between fluorinated groups, to varying levels of success. This paper will summarize and discuss enantioselective methods to obtain alcohols with a fluorine atom or fluorinated groups (such as CF_3, OCF_3, and SCF_3) in β-position (also known as vicinal fluoro alcohols, or fluorohydrins, and their derivatives) developed from 2014–2025, inclusive (Fig. 2). The approaches

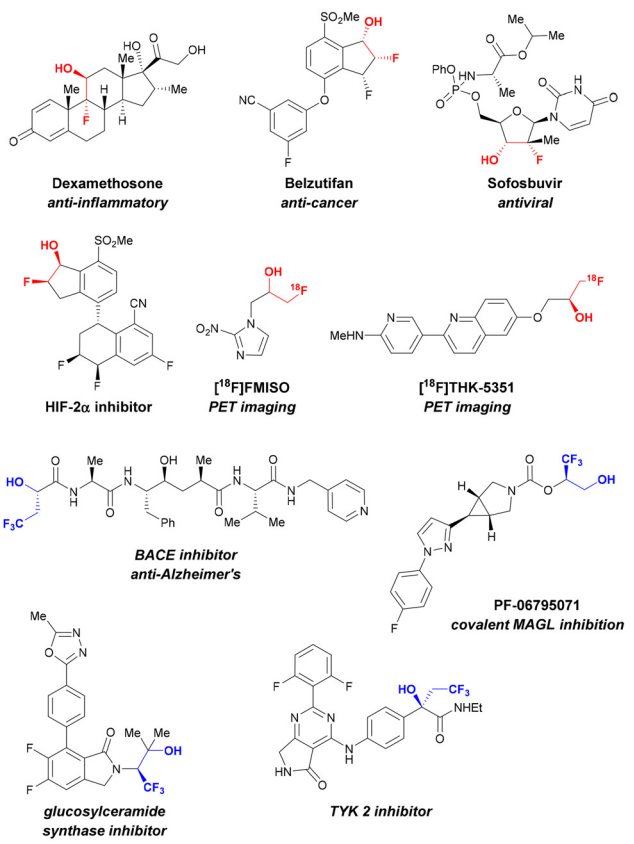

Fig. 1 Selected examples of fluorohydrin motif in bioactive compounds.

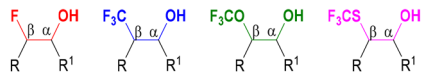

Fig. 2 Products described in this review.

are separated according to the chemical method used. Finally, selected recent examples of the synthesis of bioactive compounds will be discussed in the final section 6.

2 Reactions of carbonyls

2.1 Reductions of chiral ketones

One means of accessing chiral alcohols is to first synthesize chiral ketones which can undergo reduction. The following methods describe approaches to enantioselective α-fluorinated ketones, with examples of derivatization to the corresponding β-fluorinated alcohols.

Reyes, Vicario and coworkers reported the enantioselective cross-benzoin reaction of aldehydes and alkynones catalyzed by an N-heterocyclic carbene (NHC) to furnish tertiary alkynyl carbinols (Scheme 1).[11] Their solvent selection avoided the formation of self-benzoin or Stetter side products, and the low temperature helped achieve chemo- and enantioselectivity. Twenty examples were provided in the reaction scope, with yields between 25 and 99% with 75 to >99% ee. Aldehyde substitution included thiophene, furan, decorated phenyl, cyclopropyl, and alkyl chains. The alkynyl ketones were not limited to activated substrates (trifluoromethyl was replaced with methyl or ethyl groups), and varying aromatic, heteroaromatic, aliphatic, and silyl groups adorned the alkyne moiety. Subsequent diastereoselective reduction by Red-Al® afforded an allylic β-CF_3 alcohol motif, with absolute configuration determined by X-ray analysis. Alternatively, under Luche

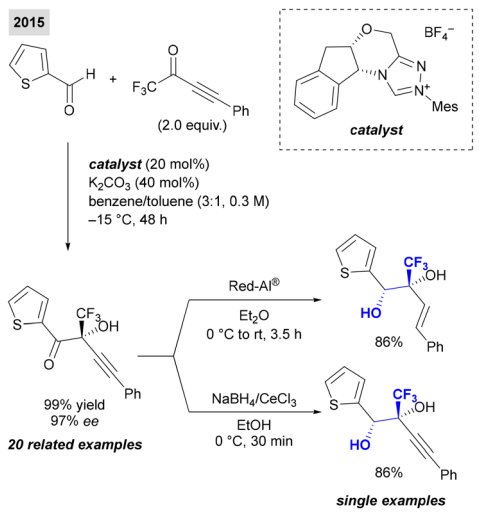

Scheme 1 Enantioselective cross-benzoin reaction of aldehydes and alkynones catalyzed by an N-heterocyclic carbene (NHC).

reduction conditions afforded the alkynyl β-CF_3 alcohol diastereoselectively. Both subsequent transformations retained the enantioselectivity of the starting ketone.

Cahard and coworkers described the synthesis of enantiopure β-SCF_3 alcohols using Evan's chiral oxazolidinone auxiliary (Scheme 2).[12] The mechanism proceeds through the major (*Z*)-lithium imide enolate. The less sterically hindered *re* face of the enolate attacks the electrophilic N-SCF_3-phthalimide, resulting in a diastereoselective α-trifluoromethylthiolation. Ten successful examples of aliphatic substrates were described (58–85% yield, 63 : 37 to 100 : 0 dr) and eight examples of aromatic substrates (56–84% yield, 70 : 30 to 98 : 2 dr). Diastereomeric ratio was enhanced by chromatography, after which two examples were provided of cleavage of the chiral auxiliary to access the target alcohols without racemization.

J. Wang and coworkers described a catalytic asymmetric trifluoromethylthiolation protocol to access α-SCF_3 ketones enantio- and diastereoselectively (Scheme 3).[13] This proceeded *via* a copper-catalysed tandem 1,4-addition trifluoromethylthiolation onto acyclic enones, with SCF_3-4-nitro-phthalimide as the SCF_3 source. Across 22 examples of ketones, the yields ranged from 50–92%, with a diastereoselectivity between 1 : 1 to 20 : 1 dr, and enantioenrichment of 0–96% ee. Subsequent transformations included reduction by L-Selectride and methyl Grignard addition to access the β-SCF_3 alcohol motif.

J. Wang reported the catalytic asymmetric synthesis of α-trifluoromethyl cycloheptanones. This occurred by a homologation reaction of cyclic ketones with CF_3CHN_2 serving as both the trifluoromethyl and carbon source (Scheme 4).[14] A Sc(III) catalyst was employed with a chiral bisoxazoline ligand. Anhydrous conditions proved necessary to avoid coordination of water to the Sc(III) that would decrease the catalyst's Lewis acidity. The desymmetrization reaction showed generally good diastereoselectivity and enantioenrichment: a series of 21 successful cycloalkanones substrates demonstrated 51–88% yield, up to 20 : 1 dr, and 6–95% ee, and ten examples of silacyclohexanones showed 53–87% yield, up to 7 : 1 dr, and 71–94% ee. The synthesis was performed on gram-scale, with further derivatization that afforded cyclic β-CF_3 alcohols in two examples by reduction of the ketone.

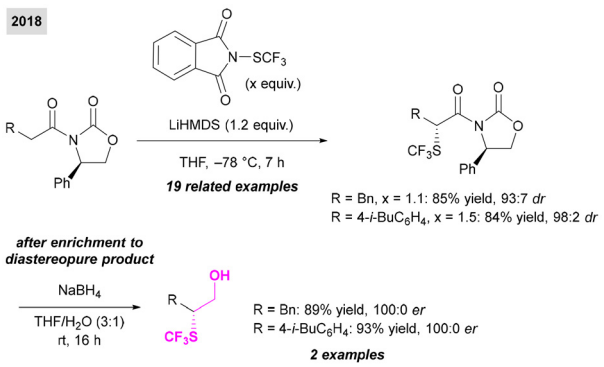

Scheme 2 Synthesis of enantiopure β-SCF_3 alcohols using Evan's chiral oxazolidinone auxiliary.

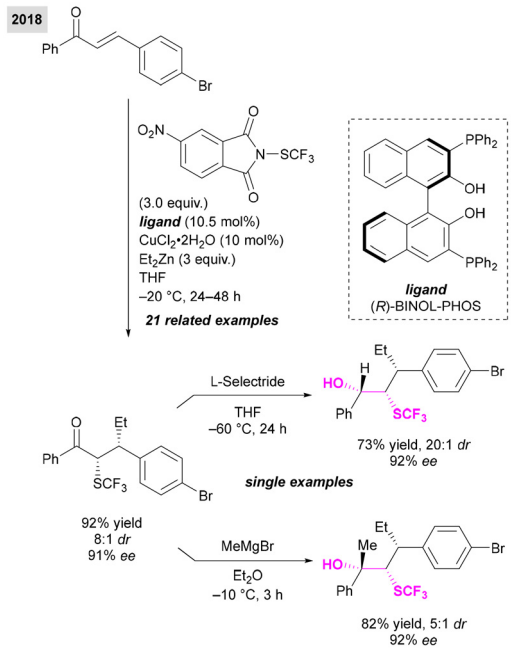

Scheme 3 Asymmetric trifluoromethylthiolation of acyclic enones.

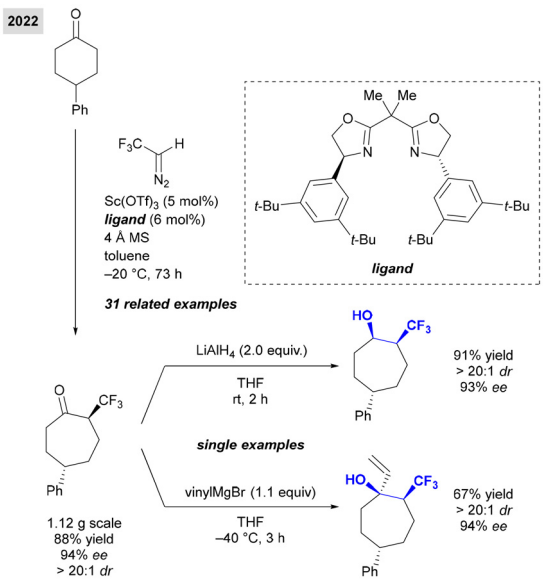

Scheme 4 Sc(III)-catalysed asymmetric synthesis of α-trifluoromethyl cycloheptanones.

X.-S. Wang and coworkers reported an asymmetric nickel catalyzed reductive cross coupling to form enantioenriched α-CF_3 ketones (Scheme 5).[15] Acyl chlorides were coupled with a racemic trifluoromethylated alkyl bromide under nickel catalysis in the presence of a chiral bioxazoline ligand. The resulting ketones could then be isolated (40 examples) or reduced by sodium borohydride in methanol in one pot to give the corresponding β-CF_3 alcohol in high ee across a variety of substrates

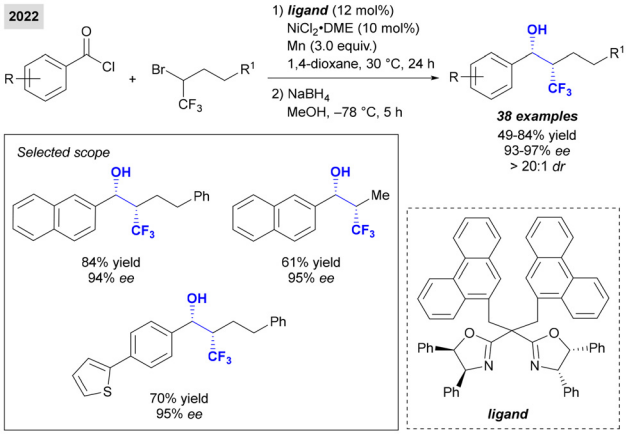

Scheme 5 One pot asymmetric nickel-catalysed reductive cross coupling of acyl chlorides and racemic trifluoromethylated alkyl bromide, and subsequent reduction.

(38 examples). Yields ranged from 49–84%, with enantioenrichment between 93–97% ee and >20 : 1 dr for the alcohols.

Around the same time, L.-A. Chen and coworkers published a related study of asymmetric nickel catalyzed reductive cross coupling to afford α-CF_3 ketones (Scheme 6).[16] Acyl chlorides and bromides were reacted with racemic α-CF_3 alkyl bromides. The nickel catalyst, chiral bisoxazoline ligand, and ancillary phosphine ligand improved enantiocontrol and manganese served as a reductant. The proposed radical mechanistic model invoked stereoinduction through a pentacoordinated Ni (III) complex transition state. The preferred conformation in this transition state would orient the substrate's bulkier alkyl hemisphere away from the ligand phenyl group. The trifluoromethyl group would also need to be positioned away from the phenyl group, so the preferred conformation would have the α-hydrogen proximal to the phenyl. Of the 37 examples of enantioenriched α-CF_3 ketones in the reaction scope, two products underwent reduction to form the β-CF_3 alcohol motif in high enantioselectivity (94 : 6 and 94.5 : 5.5 er).

In a campaign to apply N-heterocyclic olefins (NHOs) – which are known for their strong basicity and high nucleophilicity – as asymmetric organocatalysts, Dong described the enantioselective α-functionalization of β-ketoesters (Scheme 7).[17] Comparable amination and trifluoromethiolation protocols were reported. Control experiments and computational studies indicated that the stereoselectivity might be due to base and dual hydrogen-bonding activation. Of note to the current review, the enantioselective trifluoromethiolation was demonstrated across 22 substrates in 55–99% yield and 58–90% ee. Further transformations of the reported products were reported. Notably, two examples of the methyl Grignard reagent addition to the trifluoromethiolation products afforded the corresponding β-SCF_3 alcohols in 90% yield and 82–90% ee.

Y. Chen, Z. Wang and coworkers described an asymmetric [1,3] O-to-C rearrangement to form quinolinones under copper (II) catalysis with a bisoxazoline ligand (Scheme 8).[18] The proposed mechanism involves coordination of the substrate to the copper(II) catalyst, forming a tetrahedral species, which induces facial selectivity for the intramolecular rearrangement. The investigated 4-trifluoromethyl quinolinones underwent a subsequent reduction step to form the desired alcohols. The transformation on the eight examples in this series was achieved in 72–99% yield, 93–98% ee, and >19 : 1 dr.

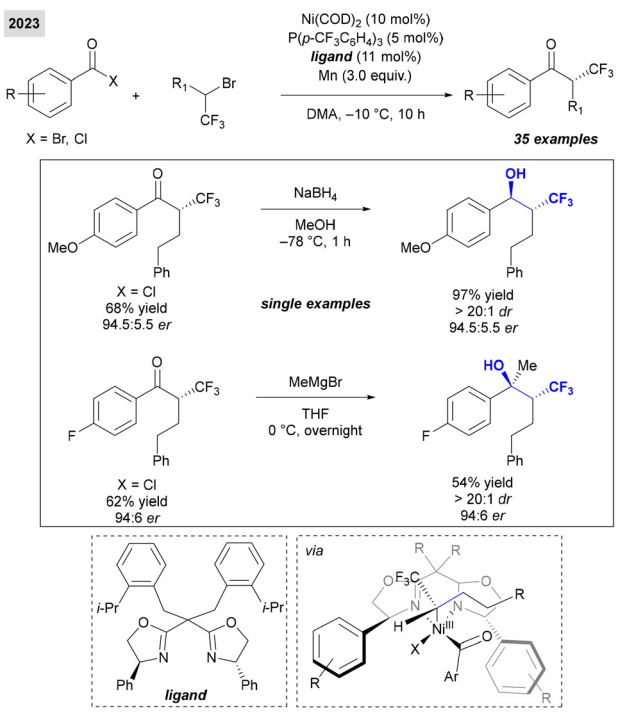

Scheme 6 Asymmetric nickel catalyzed reductive cross coupling of acyl chlorides and racemic trifluoromethylated alkyl bromide, and further derivatization of products.

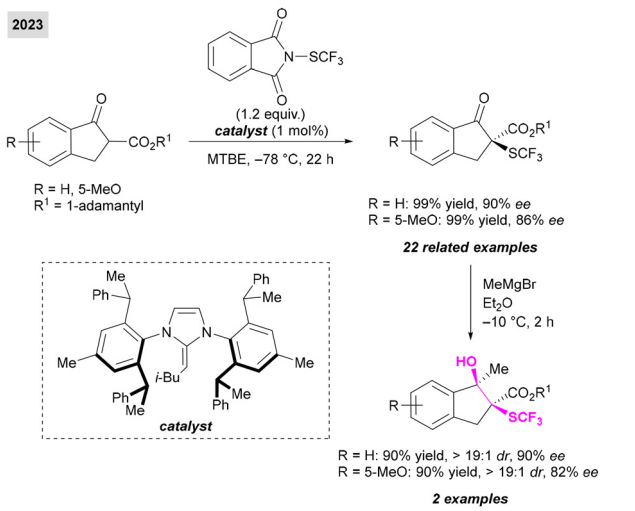

Scheme 7 Organocatalytic asymmetric trifluoromethiolation and subsequent reduction of products.

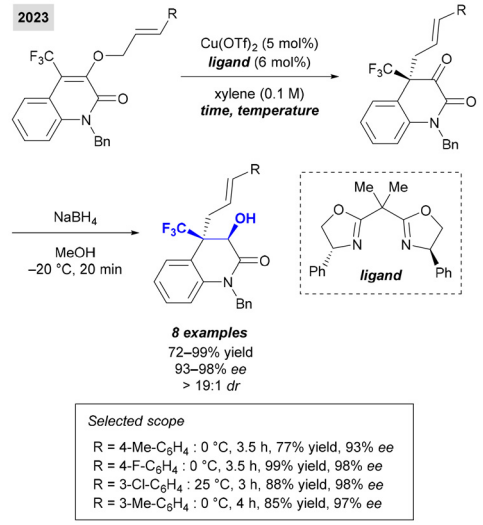

Scheme 8 Cu(II) catalysed asymmetric [1,3] O-to-C rearrangement and subsequent reduction of products.

2.2 Chemical asymmetric reductions of prochiral ketones

Prochiral ketones can undergo enantioselective reduction to yield the chiral fluorohydrin motif. Further discussion of the asymmetric transfer hydrogenation of other fluorinated ketone and imine substrates has been explored by Phansavath, Ratovelomanana-Vidal and coworkers.[19] Meggers and coworkers investigated the use of a chiral-at-metal iridium catalyst to perform photoredox and asymmetric transfer hydrogenation reactions in one pot (Scheme 9).[20] Through first a photoredox-catalyzed radical trifluoromethylation using Togni's reagent with compact fluorescent light onto electron-rich silyl enol ethers, α-CF_3 ketones were generated. The asymmetric transfer hydrogenation proceeded with the same iridium catalyst to afford four examples of β-CF_3 alcohols in overall 76–81% yield and 91–94% ee.

Competing enantioselective conversion (CEC) is a means of inferring the absolute configuration of a molecule. By running the same reaction with a chiral catalyst or reagent with each enantiomer separately and then comparing the conversion of each enantiomer at a given time point, it is possible to determine the absolute configuration based on previously reported information on relative reactivity. Birman's chiral acylating homobenzotetramisole (HBTM), performs an enantioselective acylation reaction which can be used for kinetic resolution, but typically requires a π-system to enable enantioselectivity. Rychnovsky and coworkers described their work towards applying Birman's HBTM towards a CEC protocol, which utilises heteroatoms as directing groups instead of the prototypical aromatic groups (Scheme 10).[21] They determined, among other findings, that halogens, and, most prominently, a fluorine atom, could be used as directing groups. They hypothesized that the polarized C–F bond interacted with the cationic catalyst, and that the reaction proceeded faster when the alkyl group was oriented towards the least sterically congested environment, in the proposed transition state.

Thomas and coworkers reported an example of catalytic enantioselective hydroboration of ketones (Scheme 11).[22] Typical hydroboration protocols require stoichiometric quantities of enantioenriched borane reagent which is often destroyed during the reaction. However, the authors reported a catalytic Midland reduction that ensured catalytic turnover through a boron–oxygen transborylation of 9-borabicyclo[3.3.1]nonane (9-BBN) and β-pinene using H-Bpin to perform the turnover. The title boron–oxygen transborylation was proposed to have occurred *via* a concerted, stereoretentive σ-bond meta-

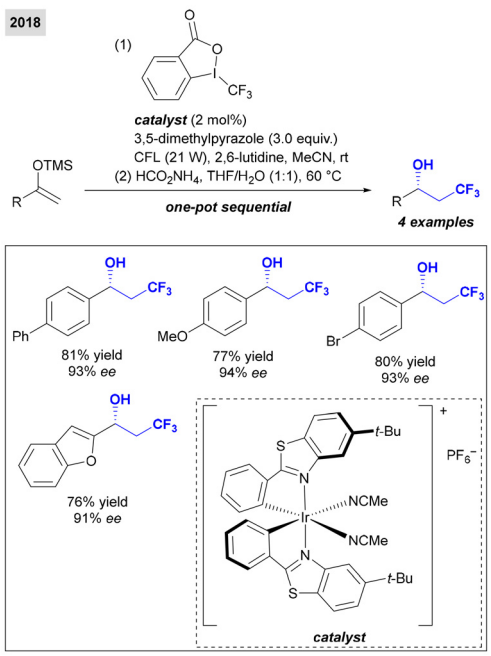

Scheme 9 Photoredox radical trifluoromethylation and asymmetric transfer hydrogenation by chiral iridium catalysis.

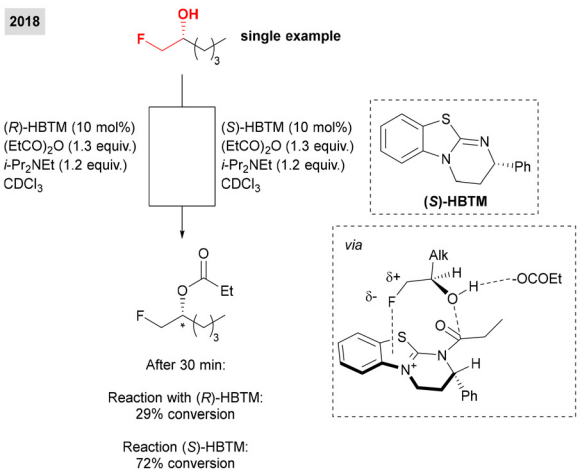

Scheme 10 Competing enantioselective conversion (CEC) with Birman's homobenzotetramisole (HBTM) chiral acylating agent.

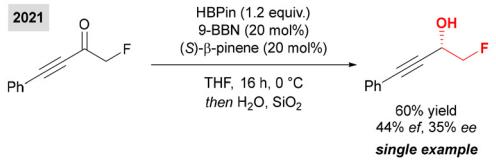

Scheme 11 Catalytic enantioselective hydroboration of ketones.

thesis mechanism. While a lower level of enantiofidelity (reported as "ef", defined as a measure of enantioenrichment retained when performing the reaction with substoichiometric quantities of catalyst relative to with stoichiometric quantities) was observed for the fluorinated substrate in Scheme 11, the method had overall modest to good yield and enantioenrichment (32–80% yield and 34–91% ee overall across 25 substrates).

Shao, X. Zhang and coworkers reported the asymmetric hydrogenation of fluorinated ketones (Scheme 12).[23] They employed an iridium catalyst $[Ir(COD)Cl]_2$ and a ferrocene-based tridentate chiral ligand with H_2 gas. Their scope primarily consisted α-CF_3 alcohols, including substrates towards the syntheses of Odanacatib and LX-1031. Other fluorinated groups were also tested, producing β-F alcohol (92% yield, 99% ee), α-CF_2H alcohol (99% yield, 99% ee), and α-$CF_2CF_2CF_3$ alcohol (97% yield, 87% ee).

Cotman and coworkers reported their enantioselective synthesis of β-CF_3, β-SCF_3, and β-OCF_3 alcohols *via* a ruthenium-catalysed Noyori-Ikariya asymmetric transfer hydrogenation dynamic kinetic resolution (ATH-DKR) (Scheme 13).[24] The reaction was applied to 13 cyclic CF_3 substrates, with yields between 37 to >99% and enantioselectivities from 45 to >99%. The conditions tolerated varied ring size (5, 6, 7 membered) and substituents (CF_3, halogen, and methyl ether, but lower yield for protected amine). An acyclic CF_3 substrate was attempted in good 97.5% ee, but 80 : 20 dr. One cyclic OCF_3 and two cyclic SCF_3 substrates were demonstrated, and one 1-SCF_3-2-indanone substrate was attained in 99% yield, but 45% ee. The resulting alcohols were subjected to further transformations (Friedel–Crafts benzylation, conversion to amine, propargylation, Suzuki cross coupling, and oxidation to ketone) with retention of stereochemistry. As such, this method is versatile for a variety of fluorinated groups (CF_3, OCF_3, SCF_3), but is limited to carbonyls adjacent to aromatic groups, and diastereoselectivity suffers in the case of acyclic substrates. Seven SCXRD were obtained and DFT studies were performed to offer mechanistic insights.

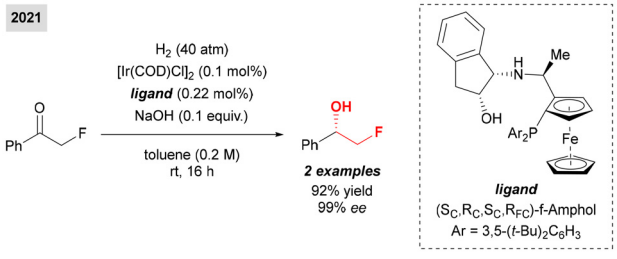

Scheme 12 Asymmetric hydrogenation of fluorinated ketone by iridium and chiral ferrocene catalysis.

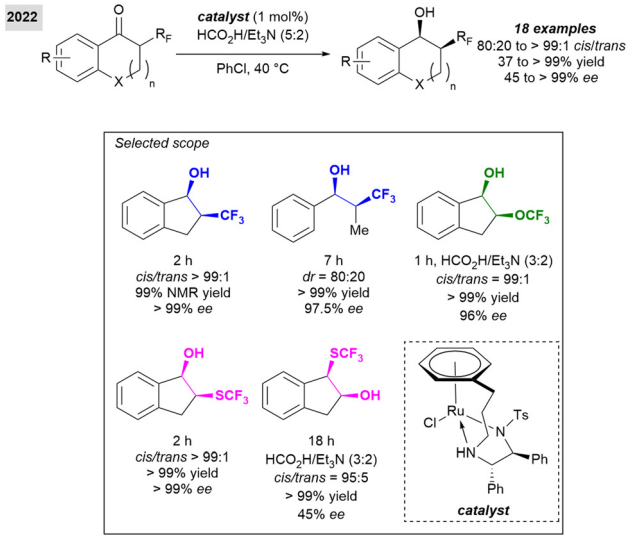

Scheme 13 Noyori–Ikariya asymmetric transfer hydrogenation dynamic kinetic resolution (ATH-DKR) of ketones and selected scope examples.

Phansavath, Ratovelomanana-Vidal and coworkers published a series of reports in the past years describing their efforts towards the asymmetric transfer hydrogenation (ATH) dynamic kinetic resolution (DKR) of various cyclic substrates. The authors disclosed the Ru(III)-catalyzed ATH-DKR of eleven examples of 3-fluorochromanone derivatives in 80–96% yield, with 92 : 8 to 99 : 1 dr and 92 to >99% ee (Scheme 14A),[25] with successful demonstration of scale up. The proposed transition state invokes edge-to-face stabilization by the catalyst's η^6-arene and π-system of substrate ($C(sp^3)$–H/π-interaction), as well as interaction between the ligand's N–H–O═C bond and CH–π interaction. The same authors applied the technology to ten examples of *N*-Boc-3-fluoro-dihydrotetrahydroquinolin-4-ones in 70–97% yield, 94 : 6 to 99 : 1 dr, and over 99% ee (Scheme 14B).[26] In this instance, they employed a tethered Ts-DENEB ligand due to the higher diastereoselectivity and enantioselectivity that it achieved. Electron withdrawing halide and trifluoromethyl substituents were well tolerated, as was methyl substitution, but slightly lower diastereoselectivity was achieved with 7-methoxy substitution, and 6,7-dimethoxy substitution required higher catalyst loading and reaction time. The reaction was demonstrated on a gram scale successfully, and further derivatization included cleaving the Boc protecting group. Phansavath, Ratovelomanana-Vidal and coworkers disclosed a Rh(III)-catalysed dynamic kinetic resolution asymmetric transfer hydrogenation to achieve enantioenriched CF_3-chromanol, thiochromanol, tetralol, and indanol derivatives (Scheme 14C).[27] The authors applied HCO_2H and Et_3N as the hydrogen source and used a Rh catalyst due to its augmented reaction time (100% conversion after 10 min) compared to two

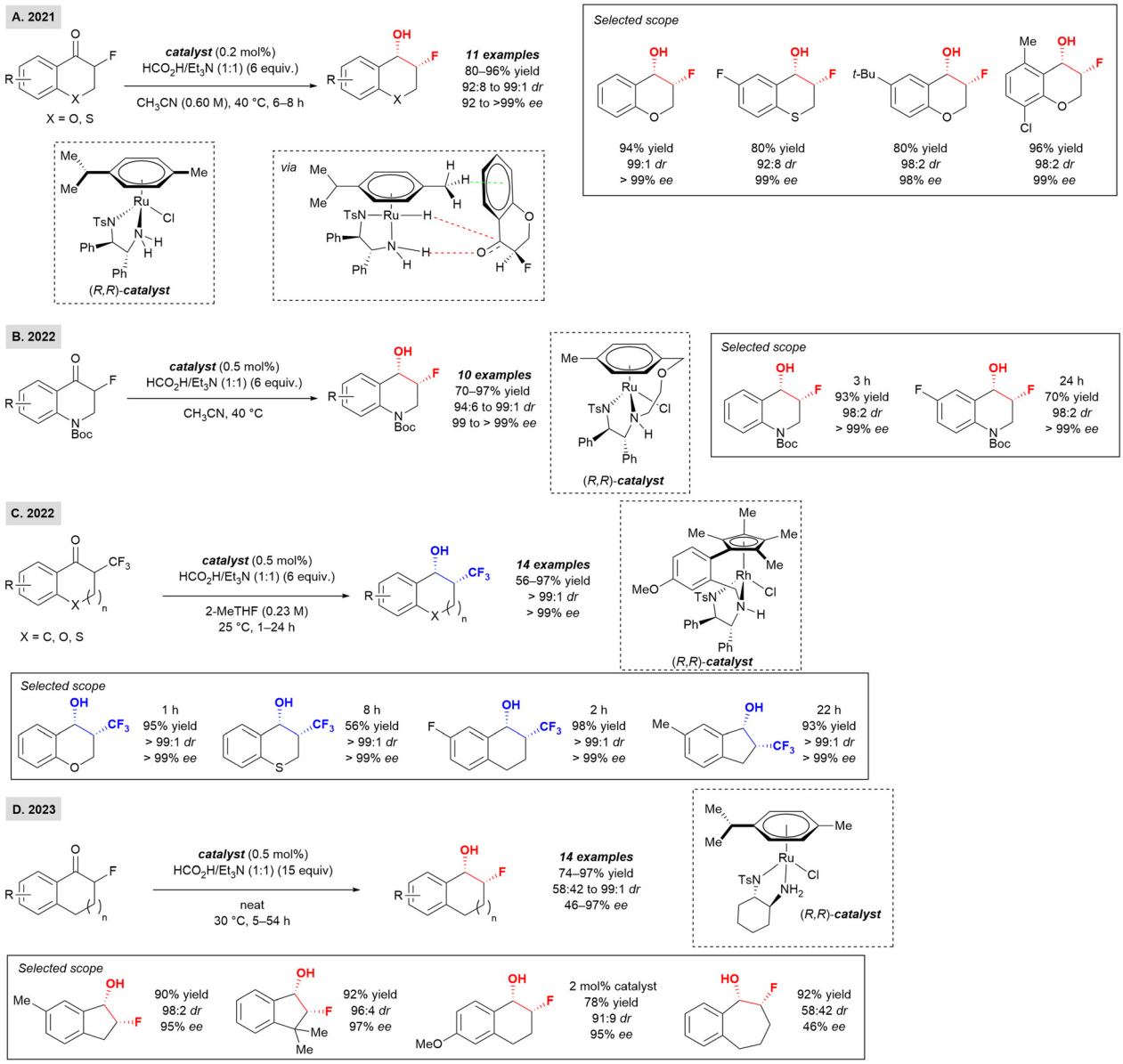

Scheme 14 Rh(III)-catalysed dynamic kinetic resolution asymmetric transfer hydrogenation towards achieve enantioenriched CF_3-chromanol, thiochromanol, tetralol, and indanol derivatives.

commercially available Ru catalysts. The product alcohols were all attained in >99 : 1 dr and >99% ee. Both electron withdrawing and donating groups were well tolerated for chromanone substrates, with 91–97% yield. The thiochromanone example required a higher catalyst loading to attain a yield of 56%. Tetralones were achieved in 90–98% yield and indanones were met with similar success (90–97% yield). An X-ray structure was obtained to determine the absolute configuration of products. The reaction was scaled up to 1 g scale, and further synthetic steps were performed to derivatize products. For their next act, the authors performed a ruthenium-catalysed ATH-DKR to afford 14 examples of 3-fluorochromanols, 3-fluorotetrahydroquinolinols, 2-fluoro inden-1-ols, and 2-fluoro 1,2,3,4-tetrahydronaphthalen-1-ols (Scheme 14D).[28] Yields ranged from 74–97%, with 58 : 42 to 99 : 1 dr and 46–97% ee. The primary focus of this paper was to perform a subsequent deoxofluorination step with DAST to afford the difluorinated species.

Noyori-Ikiraya catalysts typically rely on the CH/π interaction between the electron poor η^6-arene of the chiral ligand with the π electrons of the ketone substrate to transfer stereochemical information. Cotman and coworkers performed computational studies to determine the stereoselective influence of the SO_2 H-bond acceptor unit of the catalysts and the CH/π interactions.[29] They found that these interactions can enable ketones with an α-positioned H-bond donor to receive stereochemical guidance from the SO_2 unit. As such, the authors investigated the hydrogen-bonding effects of different Noyori-

Ikiraya catalysts in the dynamic kinetic resolution of α-hydroxy-α-CF_3 ketones (Scheme 15). The reaction to form CF_3-substituted-*syn*-1,2-diols functioned well for both electron withdrawing and donating substrates, but that electron rich substrates required higher catalyst loading. Regarding functional group tolerance, an aldehyde moiety was concomitantly reduced, and 16% of saturated side product was detected in the reduction of an α,β-unsaturated ketone. A single crystal XRD was obtained to determine the absolute configuration of products. Benzyl substituted ketones were reduced selectively. An alkyl substrate was reduced with 63% yield, 90 : 10 *syn*/*anti*, and 98% ee. The success of this alkyl substrate was attributed to hydrogen bonding between either the substrate $CF_3CH(OH)$ to the catalyst SO_2, or between the CF_3 and η^6-arene ligand. Further synthetic derivatization afforded biologically relevant motifs, such as a glycogen phosphorylase inhibitor and a topoisomerase inhibitor ULD1 analogue.

Švenda[30] and coworkers described the modulated stereoselective effect of a methoxyimino group on the asymmetric transfer hydrogenation (ATH) of α-methoxyimino-β-keto esters compared to β-keto esters (Scheme 16). This further study was performed considering initial results[31] discussed in their route to (+)-Actinobolin, wherein they noted an enhancement in enantioenrichment due to the presence of the methoxyimino group. In the synthesis of the β-CF_3 alcohol, asymmetric reduction followed by cleavage of the methoxyimino group afforded enhanced specific rotation, from $[\alpha]_D$ = +8 by Route A to $[\alpha]_D$ = +16 through the methoxyimino path Route B. A similar effect was shown for most substrates, including the β-CHF_2 alcohol, which was nearly racemic through the direct Route A, to $[\alpha]_D$ = +21 through Route B. However, a reversal of stereochemistry was observed in the example of the β-CH_3F_2 alcohol, with higher enantioselectivity observed when using the *Z*-methoxyimine isomer. Computational studies suggested

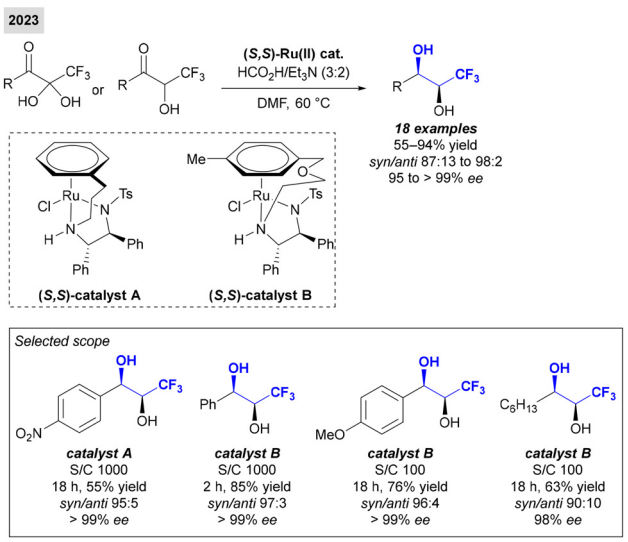

Scheme 15 Study of Noyori–Ikiraya catalysts in the dynamic kinetic resolution of α-hydroxy-α-CF_3 ketones.

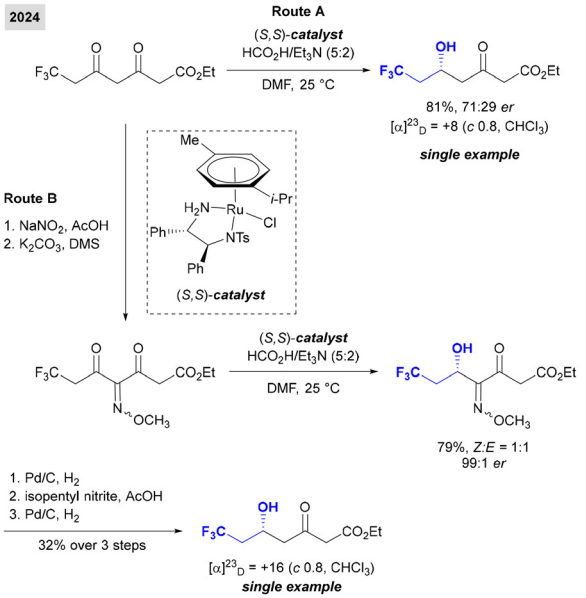

Scheme 16 Stereoselective effect of a methoxyimino group on the asymmetric transfer hydrogenation (ATH) of α-methoxyimino-β-keto esters.

that transition states with minimized SO_2-substrate repulsion and attractive η^6-arene ligand and substrate interactions contributed to enantioselectivity.

2.3 Enzymatic asymmetric reductions of prochiral ketones

As an alternative to transition metal catalysts, biocatalysts can be applied to reactions either as isolated enzymes with a cofactor, or as whole cell systems. The innate chirality of these biocatalysts can be leveraged for asymmetric transformations.

Alsafadi, Paradisi and coworker disclosed an enzymatic ketone reduction by the halophilic alcohol dehydrogenase ADH2 from *Haloferax volcanii* (*Hv*ADH2), using an NADPH cofactor that was regenerated by ethanol (Scheme 17).[32] This enzyme was found to be active and stable in organic solvents, and was immobilized on a solid support for easy recovery and reuse. This enzyme follows Prelog's rule,[33] as do most alcohol dehydrogenases. Of interest here is the single example of α-fluoroacetophenone substrate, which was here delivered in >99.9% conversion and >99% ee (*S*) – the highest performing substrate in the tested series. It had higher conversion than the related α-chloro acetophenone (94% conversion, >99% ee

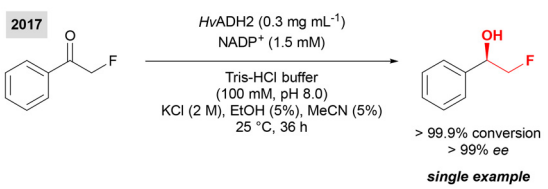

Scheme 17 Reduction of aromatic fluoro-ketone by halophilic alcohol dehydrogenase ADH2 from *Haloferax volcanii* (*Hv*ADH2).

(*S*)-) and the α-bromo acetophenone (38% conversion, >99% ee (*S*)-), which the authors attribute to fluorine's size and electronegativity.

Q. Wu developed a one-pot, two-enzyme, three-step process to enantioselectively generate β-fluoro alcohols from β-ketonic esters (Scheme 18).[34] The β-ketonic ester substrates were hydrolysed by a lipase to generate β-keto acids, followed by a spontaneous decarboxylative fluorination using Selectfluor. The resulting α-fluorinated ketones were next reduced to either the (*R*)- or (*S*)-enantiomer depending on the applied ketoreductase (KRED). Despite the highly oxidizing nature of Selectfluor, it was found to be compatible with the selected enzymes. Both the CAL-B enzyme and Selectfluor were necessary to be present for the first part of the cascade to proceed. Excess Selectfluor was essential to pushing the equilibrium of the reaction forward and forming the fluorinated products, especially for less reactive substrates. The conversions (determined by GC) for the first two steps (1 and 2) were reported for 12 aromatic substrates, with conversions in the ballpark of 23–95%. This method worked particularly well for the 4-methyl acetophenone (95% conversion) and acetophenone (92% conversion) substrates, but lower conversions were determined for 4-bromoacetophenone (23% conversion), 4-chloroacetophenone (50% conversion), 2-chloroacetophenone (54% conversion) derivatives. For the asymmetric reduction step, the (*S*)-alcohol selectivity was obtained using the carbonyl reductase from *Kluyveromyces thermotolerans* (KtCR) (20–92% yields, 99% ee) and (*R*)-alcohol selectivity was obtained with the NADPH-dependent aldo–keto reductase from *Bacillus* sp. ECU0013 (YtbE) with a similar degree of success for most substrates (12–84% yield, 4–99% ee). However, in the cases of the 2-bromoacetophenone derived substrate, YtbE delivered the (*S*)-substrate instead with high selectivity (95%), and the thiophene substrate demonstrated poor (*S*)-selectivity. Whole cell cultures of the KREDs were applied to regenerate cofactors *in situ* instead of requiring additives.

Hartwig reported an enantioselective whole cell enzymatic ketone reduction using a silane as a hydride donor (Scheme 19).[35] Whole cell *E. coli* expressing human carbonic anhydrase II (hCAII) served as the biocatalyst for the reaction. In typical biological systems, carbonic anhydrase enzymes convert CO_2 to carbonic acid by a hydroxyl transfer from the enzyme's active site, which contains a zinc hydroxide. In their report, the authors introduced an abiotic silane reagent, with the aim of replacing the hydroxide at the zinc center with a hydride to perform a reduction instead. Through control experiments and computational studies, the authors ascertained that a different mechanism is at play, wherein the hydride is transferred from the silane, to the zinc center, and in turn to the ketone. The authors reported 26 examples of chiral alcohols, with substrates including heterocycles and various aromatic substitution patterns and electronics. The yields were generally high, ranging from 37 to >99% and enantioselectivities also were generally excellent from 10 to >99%, with low enantioselectivity in only the 2-bromoacetophenone substrate, likely due to the formation of a competing halogen bond at the active site. Notably, in the scope, an example of a β-F alcohol was demonstrated in >99% yield and >99% ee.

Langer, Von Langermann[36] and coworkers described the enzymatic reduction of picoline derivatives to generate enantioenriched heteroaromatic alcohols (Scheme 20). With the alcohol dehydrogenase from *Lactobacillus kefir* in a buffered system, two examples of β-F alcohols were generated

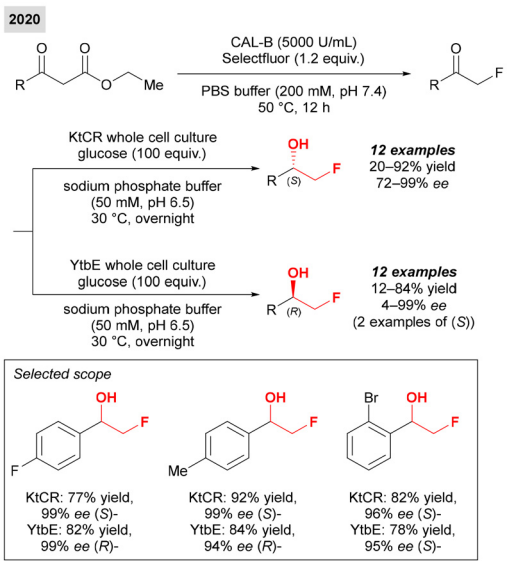

Scheme 18 One-pot, two enzyme process for the generation of either enantiomer of aromatic β-fluoro alcohol, with selected scope examples.

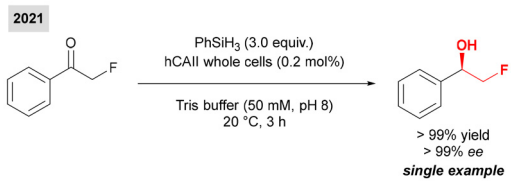

Scheme 19 Reduction of ketones by zinc metalloenzyme and silanes, regenerated by whole cells.

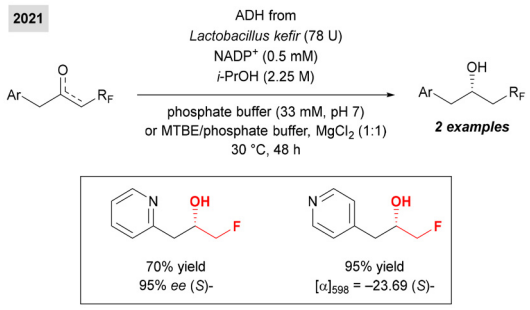

Scheme 20 Enzymatic reduction of picoline derivatives to generate enantioenriched heteroaromatic alcohols.

in 70–98% yield. Products were shown to be stable to decomposition and racemization when stored below 0 °C.

X. Chen, Xie and coworkers reported an enantioselective one-pot cascade approach to β-fluoro alcohols from styrene analogues (Scheme 21).[37] First, a photo-oxidative fluoridation proceeded with Selectfluor as the fluoride source and sodium anthraquinone sulfonate as the photocatalyst. The subsequent bio-reduction step involved either of the enantiocomplementary enzymes, alcohol dehydrogenase from *Rastonia* sp. (*Ras*ADH) or carbonyl reductase from *Kluyveromyces thermotolerans* (*Kt*CR), depending on the desired enantiomer (typically (*R*)- and (*S*)-selective respectively), with whole cell regeneration of NADPH. The proposed mechanism involved electrophilic fluorination of the styrene by Selectfluor, followed by water hydroxylation. The photooxidation step proceeded *via* a benzyl radical intermediate to generate the ketone. GC yields for the formation of α-fluoroketones ranged from 2–96%, with decomposition observed for 2- and 3-methoxy substrates. The bioreduction step yielded the (*S*)-enantiomer in 24–85% yield and 11–99% ee, and the (*R*)- in 53–87% yield and 33–99% ee. The overall reaction gave poor enantioselectivity for the *ortho*-Cl substrate (71–75% yield, 11–33% ee) and *para*-CF_3 (53–55% yield, 46–80% ee) but worked well for *meta*- and *para*-substituted styrenes (65–87% yield, 96–99% ee). The opposite selectivity was observed by both enzymes for the thiophene analogue, which gave 53% yield and 33% ee for (*R*)- and 53% yield and 35% ee for (*S*)-. The reaction was scaled up to 1 mmol, and cells could be reused up to three times.

Valotta, Gruber-Woelfler and coworkers disclosed a semi-continuous flow protocol for photocatalytic trifluoromethylation and enantioselective bioreduction by an immobilized alcohol dehydrogenase from *Lactobacillus kefir* to generate β-trifluoromethyl alcohols from methyl ketones (Scheme 22).[38] The continuous flow photocatalytic trifluoromethylation had been reported by Rincón, Kappe and coworkers,[39] with additional optimizations to the protocol disclosed in this work. This process invoked first the transformation of the model substrate, Eosin Y, into its silyl enol ether. Radical trifluoromethylation proceeded with white visible light irradiation onto an Eosin Y photocatalyst with triflyl chloride. These first two steps were performed in flow, but the subsequent enzymatic ketoreduction was not due to practical considerations – longer incubation time of at least an hour were required, and the slurry reaction mixture with the enzyme caused clogging issues. The space time yield (STY) for the photocatalytic step was 39.8 g L^{-1} h^{-1}, and 1.12 g L^{-1} h^{-1} for the enzymatic step using both free and immobilized enzyme. Many suggestions for further improvement were listed in the conclusion. Acetophenone was used as the model substrate for this study, and the (*S*)-alcohol was obtained in over 95% ee, with an example of 83% isolated yield using bead-immobilised enzyme.

2.4 Aldol reactions

X. Zhang, Ma and coworkers disclosed an enantioselective Aldol reaction of aldehydes with 2,2,2-trifluorodiazoethane as a nucleophilic masked trifluoroethyl source (Scheme 23).[40] Enantioselectivity was influenced by the employment of $ZnEt_2$-quinine and low reaction temperatures. Using a different quinine ligand was shown to afford the opposite enantiomer of a product. The synthesis of the diazo compound was demonstrated across a scope of 38 examples (62–92% yield, 73–92% ee), and was shown to work well for both aromatic groups with varying decorations and heteroatoms, as well as aliphatic aldehydes. Subsequent hydrogenation cleaves the diazo mask to afford the β-CF_3 alcohols, in two examples with overall good yield (75% and 53%) and enantioselectivity (86% and 90% ee respectively). The absolute configuration of a derivatized product was determined by XRD. A 1,2-diol was generated with retention of enantioenrichment through an acylation, oxidation, reduction, and deacylation pathway.

Kumagai, Shibasaki and coworkers reported an aldol reaction of α-CF_3 amides with arylglyoxal hydrates. This reaction occurred enantioselectively under Cu(I) catalysis with a chiral ferrocene-based bisphosphine ligand (Scheme 24).[41] The 7-azaindoline moiety on the amide substrates was shown to stabilize the Cu-enolate that was formed, contributing to enantioselectivity.

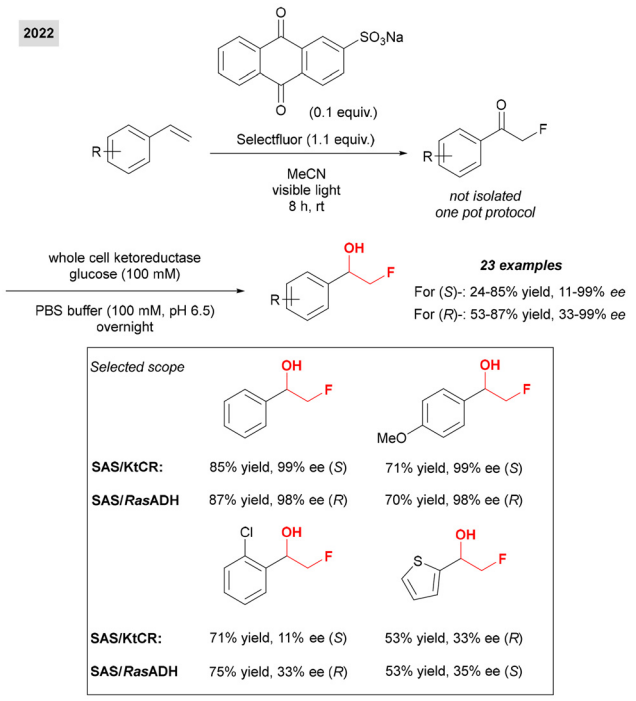

Scheme 21 One-pot photooxidative fluorination and enzymatic reduction of styrenes to β-fluoro alcohols and selected scope examples.

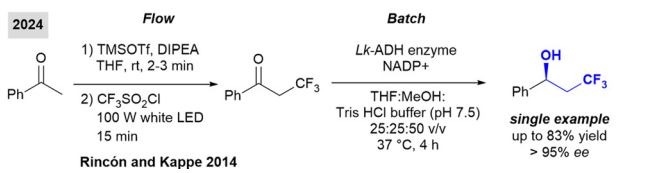

Scheme 22 Semi-continuous flow trifluoromethylation and enzymatic reduction of acetophenone.

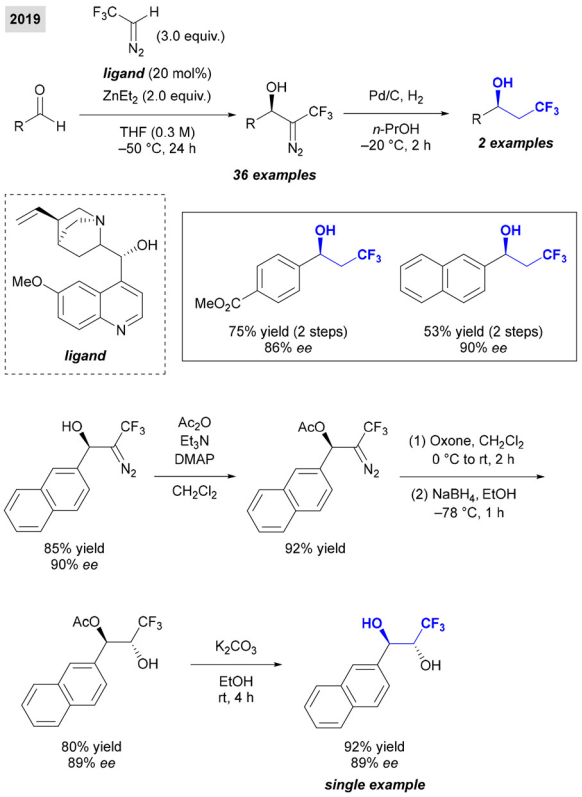

Scheme 23 Enantioselective Aldol reaction of aldehydes and a diazo-masked trifluoroethyl and subsequent reduction of two examples to the corresponding β-CF_3 alcohols.

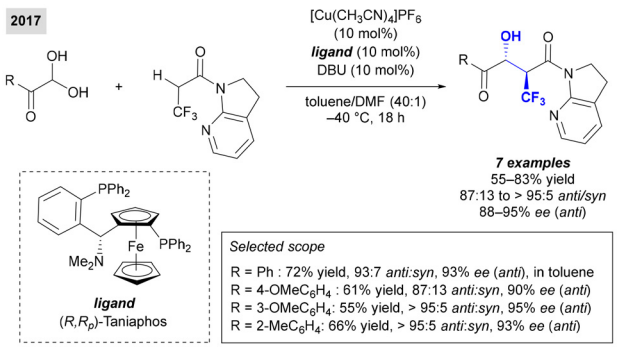

Scheme 24 Enantioselective copper-catalysed aldol reaction of α-CF_3 amides with arylglyoxal hydrates.

While nonpolar hydrocarbon solvents afforded higher enantioenrichment, solubility issues were encountered, such that DMF was added in small quantities. The scope of the reaction was extended to aromatic compounds only, as aliphatic substrates most likely encountered competitive enolization. The reaction was sensitive to the substrates' electronics, resulting in lower yields when deviating from an electron neutral substrate. *ortho*-, *meta*-, and *para*-substitution were demonstrated, as well as a thiophene unit (83% yield, >95 : 5 *anti*/*syn*, 88% ee). The reaction was demonstrated on gram scale (for the R = Ph substrate, performed in toluene, 70% yield, *anti*/*syn* = 92/8, 92% ee (*anti*)).

2.5 Asymmetric additions to prochiral ketones

Hoveyda and coworkers discussed their catalytic enantioselective addition of organoboranes to fluoroketones, with an emphasis on generating α-CF_3 alcohols (Scheme 25A).[42] Their chiral catalyst was generated *in situ* from an aminophenol, which enabled favourable electrostatic interaction between the fluorine-substituted substrates and ammonium moiety of the catalyst. However, when the authors translated this chemistry to form the β-F alcohols, they were met with decreased enantioselectivity. They explained this result by conflicting C–F and C=O carbonyl dipoles. Subsequently, Hoveyda and coworkers described the enantioselective reaction of fluorinated ketones with borylated alkenes, generating *Z*-allylic tertiary alcohols, using a valine-derived organocatalyst (Scheme 25B).[43] While much of the article pertains to the trifluoromethylated substrates, both enantiomers of three examples of fluorinated substrates were demonstrated, with opposite stereochemistry achieved by using the *E*- or *Z*-crotylboron reagent. The α-selectivity for the reaction was particularly high, since the competing 1,3-boryl shift occurs more slowly than the addition of the organoboron intermediate to the ketone. Hoveyda and coworkers pursued their work by expanding to different halogen substitution (tri-, di-, or mono-, and Cl-, Br-, or F-), to investigate for each case whether electronic or steric factors dominate in determining the stereochemical outcome of the reaction (Scheme 25C).[44] Regarding the monofluoromethyl ketones which they subjected to their enantioselective allylation conditions, they determined by modifying the $SiPh_3$ moiety of the aminophenol catalyst to a smaller *t*-Bu group that there was a marked decrease in enantiomeric ratio (91 : 9 to 65 : 35 er). Thus, it was concluded that for monofluoromethyl ketones, steric factors influence the enantioselectivity. The authors applied their conditions to the synthesis of a bioactive compound. Due to H-bonding between the triazole unit and the ammonium on the catalyst, the stereochemical outcome was underwhelming (76% yield, 69.5 : 30.5 er). As such, the authors performed the allyl addition first to an ynone substrate, and formed the triazole ring subsequently in a one-pot reaction, for overall 86% yield and 99 : 1 er.

Shen and coworkers disclosed their synthesis of enantioenriched enol silanes through a copper-catalysed reductive coupling of fluoroalkylacylsilanes and 1,3-enynes, followed by a Brook rearrangement (Scheme 26).[45] Two products of the initial reductive coupling reaction pertain to the present discussion and were generated in 81–86% yield, 98 : 2 to >99 : 1 dr, >99% ee in both instances.

3 Reactions of unsaturated carbon–carbon bonds

3.1 Oxidations of alkenes and allenes

Our group developed a regioselective Tsuji–Trost reaction under palladium nanoparticle catalysis to introduce a 4,4,4-tri-

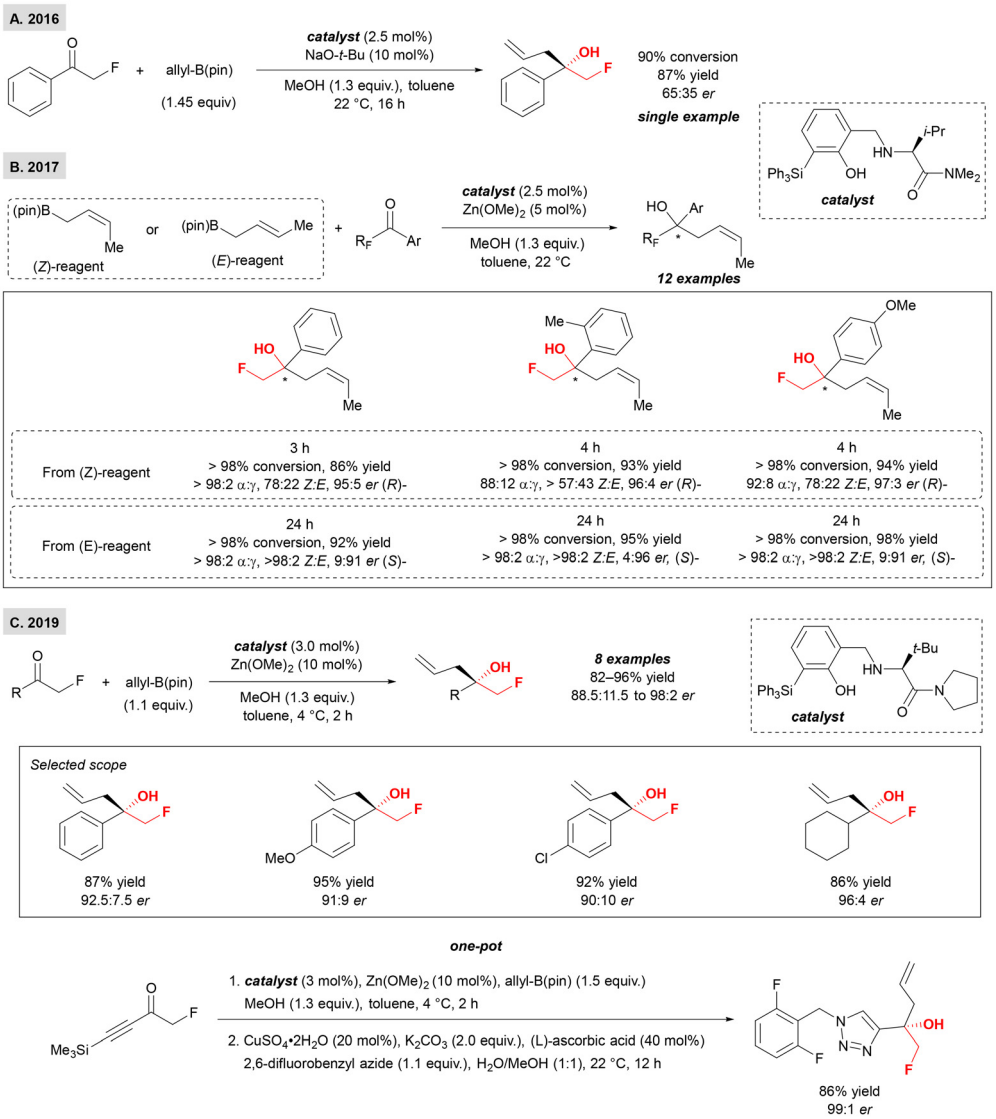

Scheme 25 Aminophenol-catalysed additions of borylated alkenes to fluorinated ketones.

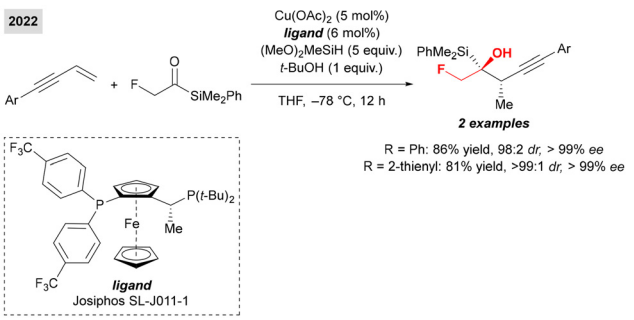

Scheme 26 Copper-catalysed reductive coupling of fluoroalkylacylsilanes and 1,3-enynes and subsequent Brook rearrangement.

fluorobut-2-ene motif onto varying nucleophiles – the first report of substitution with this chain on a nitrogen or the β-carbon of a malonate (Scheme 27).[46] Further derivatizations included an asymmetric Sharpless dihydroxylation, which yielded a trifluoromethyl diol in 86% yield and >99% ee.

X. Zhao and coworkers described in 2016 the first enantioselective alkene trifluoromethylthiolation to generate lactones from (*E*)-4-aryl-substituted but-3-enoic acids (Scheme 28A).[47] To improve the selectivity of this reaction and mitigate racemization issues, the intermediate thiiranium ion is stabilized by a bifunctional catalyst before the intramolecular cyclization step. This bifunctional catalyst comprises of a chalcogenide group serving as a Lewis base and an amine group as an H-bond donor. A new shelf stable electrophilic SCF_3 reagent, $(PhSO_2)_2N\text{-}SCF_3$, was developed as a more reactive alternative to the classical Billard's reagent, $PhNH\text{-}SCF_3$. A scope of 19 (*E*)-alkenes were tested and showed 51–93% yields, with >99 : 1 dr and 79–91% ee. An XRD was obtained for one of the product lactones to confirm absolute configuration. The mechanism of this reaction was hypothesized to proceed as follows. The Boc

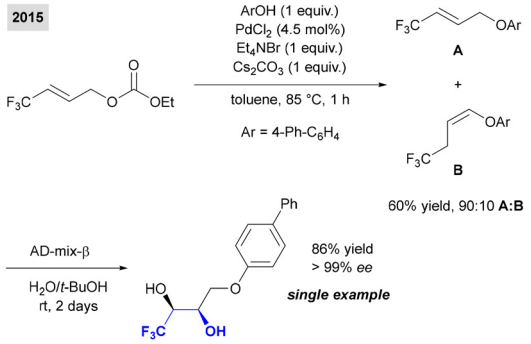

Scheme 27 Regioselective Tsuji–Trost reaction under palladium nanoparticle catalysis.

protected bifunctional catalyst is deprotected by TfOH, which in turn activates the SCF_3 reagent, transferring the SCF_3 to the bifunctional catalyst. The key step, illustrated in Scheme 28A, involves the formation of the trifluoromethylthiiranium ion with the olefin, with hydrogen bonding between the carboxylic acid of the substrate and the amine of the bifunctional catalyst. A thiiranium ion is defined[48] as an intermediate resulting from the addition of a sulfenyl group to an olefin to form a positively charged three membered ring. The TfOH is proposed to lower the acidity for the SCF_3 reagent to push the reaction forward. The final lactonization step occurs *via* intramolecular attack of the carbonyl oxygen atom to the iranium ion. Of particular interest to this paper, a single example of lactone ring opening was demonstrated, wherein the diol was generated in 92% yield, 89% ee, and 99 : 1 dr. As such, while only one example was demonstrated, this could be a simple way of achieving this motif in high *enantio-* and diastereoselectivity. Building upon the previously disclosed method, X. Zhao[49] disclosed in 2018 another means of oxytrifluoromethylthiolation of internal alkenes (Scheme 28B), this time employing a selenium catalyst and demonstrating more examples of the free alcohol. Instead of employing carboxylic acids to generate lactones, here either amides or esters were applied as directing groups to control the regioselectivity and were in turn hydrolysed to form the free alcohols. This method was shown to be a regio-, diastereo-, and enantioselective means of defunctionalizing aliphatic internal alkenes. The proposed mechanism invokes an intramolecular attack of the tethered directing group on the unstable thiiranium ion to generate a 6-membered transition state, which undergoes hydrolysis. For amide substrates, the selectivity of the reaction was highly dependent on the amide used; phthalimide performed suitably, and succinimide and saccharimide were evaluated in the substrate scope. A more sterically hindered catalyst demonstrated higher enantioselectivity. The substrate scope demonstrated six examples of alkyl chain modification in 66–98% yield, 84–94% ee, and a dr > 99 : 1 except for the pentyl chain which gave 17 : 1. Overall shorter alkyl chains performed better. Substitution on the phthalimide in the *meta* position was also explored with good selectivity. When applied to ester substrates, terminal alcohols were obtained due to an aroyl

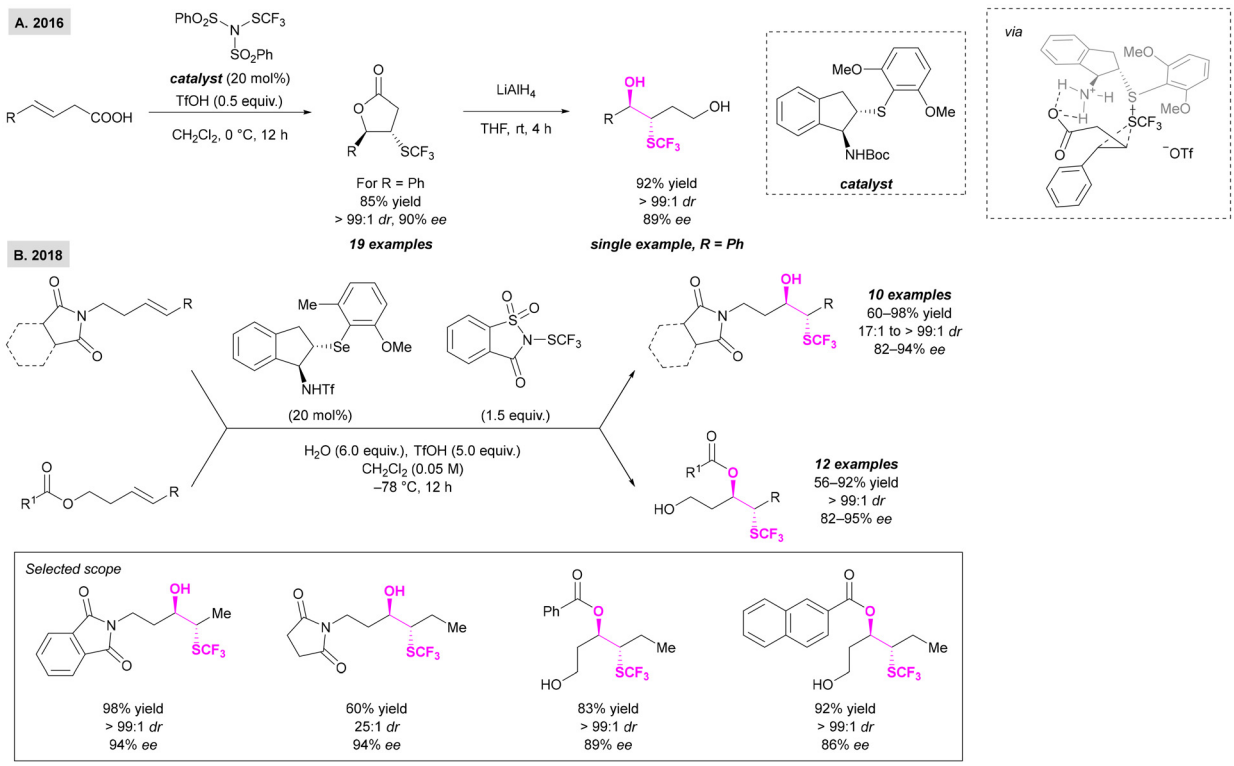

Scheme 28 Generation of SCF_3-lactones, alcohols, and esters from olefins through a key thiiranium ion intermediate.

group migration. In the scope, shorter alkyl side chains gave higher enantioselectivity, while sterically hindered groups decreased the enantioselectivity. Different ester groups were tolerated well.

Krische and coworkers described a methanol-mediated hydrohydroxymethylation of CF_3-allenes, catalysed by an iridium(I)-PhanePhos complex (Scheme 29A).[50] Fifteen examples of neopentyl alcohol products were given, in 57–95% yield and 84–94% ee. The authors determined that electron rich, electron neutral, and slightly electron deficient substrates reacted well under the following conditions: $[Ir(cod)Cl]_2$, (*R*)-PhanePhos, acetone, 70 °C. However, highly electron-deficient substrates required the use of Ir(cod)(acac), EtOAc, 80 °C. Enantioselectivity could be improved at times by adding TBAI and H_2O. Aromatic substrates were reported, but the authors claimed that alkyl substrates could also be applied, albeit with lower enantioselectivity. The X-ray structures of two products were determined to assign absolute configuration to the scope compounds. Further derivatizations were demonstrated to illustrate synthetic utility. The same group later presented a chromatographically stable, cyclometalated iridium-(*R*)-PhanePhos complex (Scheme 29B).[51] Among other reactions, they demonstrated its catalytic capabilities for their previously reported reaction of CF_3-allenes, using either a preformed catalyst or one generated *in situ*, the latter which affords higher yield likely due to counterion effects.

Jubault, Poisson and coworkers adapted the sharpless dihydroxylation for α-fluoromethylated, α,α-difluoromethylated, and α,α,α-trifluoromethylated substrates (Scheme 30).[52] Using AD-mix-α or AD-mix-β, the authors obtained both enantiomers of most α-fluoromethylated products, except for the 4-NO_2 substrate, in yields of 70–90% and between 9.5 : 90.5 to 1 : 99 er. The fifteen difluoromethylated products were obtained in 13–90% yield and 16.5 : 83.5 to 0.5 : 99.5 er on a variety of aromatic, heteroaromatic, and one aliphatic substrate, as well as one β-difluorinated substrate. Further derivatizations of the obtained products were performed to illustrate the synthetic utility of the α,α-difluoromethylated products, and the reaction was demonstrated successfully on a 4 mmol scale. The token α,α,α-trifluoromethylated substrate was demonstrated in 54–55% yield, and 0.5 : 99.5 and 99 : 1 er.

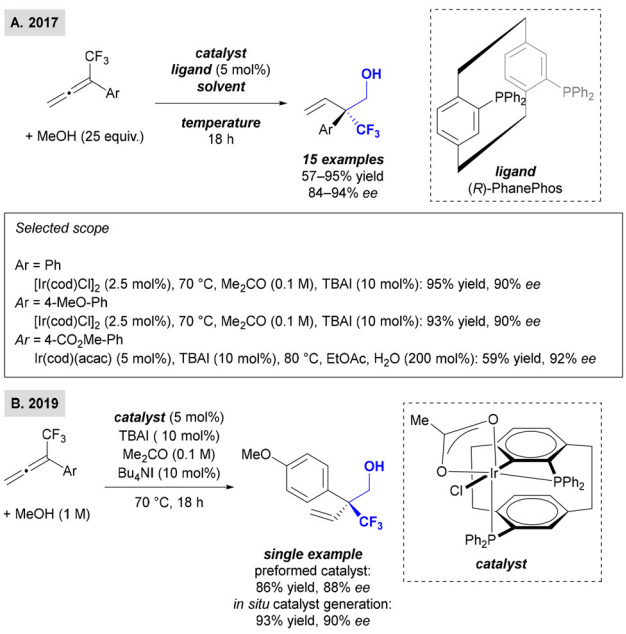

Scheme 29 Hydrohydroxymethylation of CF_3-allenes, catalysed by an iridium(I)-PhanePhos complex.

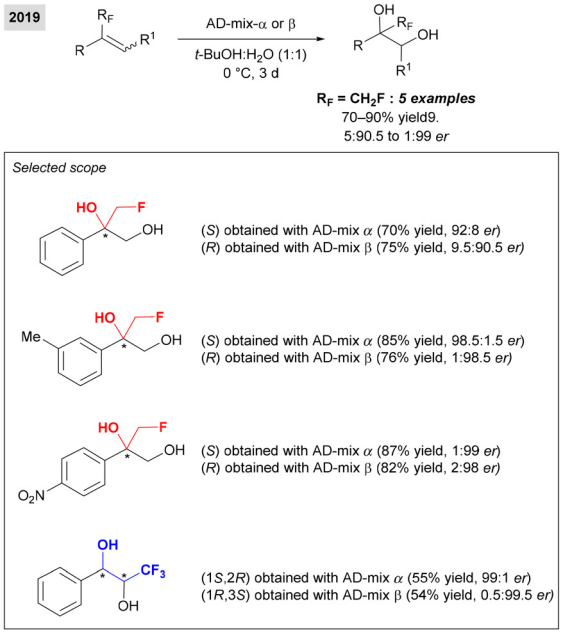

Scheme 30 Sharpless dihydroxylation towards fluorinated diols.

Yin described the three-component enantioselective synthesis of tertiary homopropargyl alcohols, of which two scope compounds pertain to the focus of the current review (Scheme 31).[53] Under copper(I) catalysis, and with NaBARF additive to ensure enantioselectivity, the asymmetric borylative propargylation of unactivated ketones with 1,3-enynes and $(BPin)_2$ was performed on 43 examples, with 61–97% yield, up to 20 : 1 dr, and 90 to >99% ee. Various aromatic, heteroaromatic and conjugated ketones, and aliphatic, aromatic, and thiophenyl alkynes were successfully demonstrated, as well as further synthetic functionalization of products.

Trost and coworkers developed a method to directly substitute α-trifluoromethyl carbanions to form pyrrolidines bearing an exocyclic alkene moiety, which upon further transformation can access the β-CF_3 alcohol (Scheme 32).[54] The authors proposed a method to stabilize α-trifluoromethyl carbanions by complexing them with a π-allyl Pd complex. The resulting zwitterions could be employed for asymmetric [3 + 2] cycloadditions to form cyclopentanes, pyrrolidines, and tetrahydrofurans. This method was demonstrated across 34 examples, in yields of 40–99%, dr ranging from 2 : 1 to > 50 : 1, and enantioenrichment of 88–99% ee. Subsequent transformations

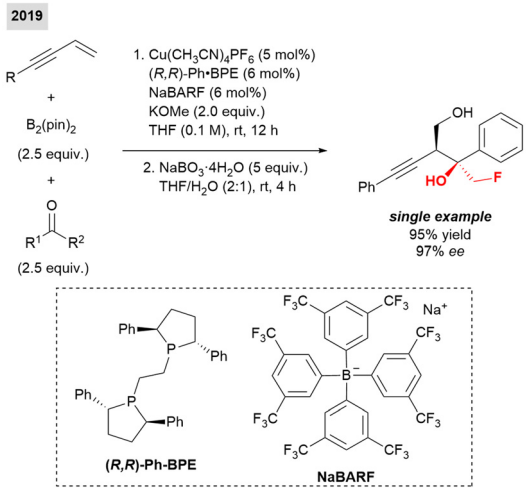

Scheme 31 Three-component enantioselective synthesis of tertiary.

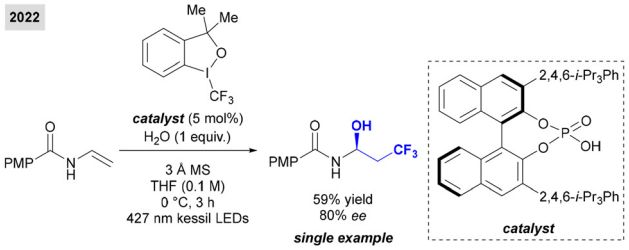

Scheme 33 Oxytrifluoromethylation by chiral phosphoric acid catalysis.

were performed on the resulting exocyclic alkene moiety of three of these such pyrrolidines to form CF_3-analogues of nicotinic acetylcholine receptor antagonists. The first example was achieved through Upjohn dihydroxylation in 92% yield, >50 : 1 dr. The next was obtained through ozonolysis and sodium borohydride reduction in 88% yield and 11 : 1 dr. The third example was obtained in the same way as the second, with an additional Boc deprotection and Eschenweiler-Clarke methylation in 67% overall yield.

H. Zheng, P.-F. Xu and coworkers disclosed an oxytrifluoromethylation reaction which generated one product of particular interest (Scheme 33).[55] The reaction invoked a chiral phosphoric acid catalyst, which under visible light conditions, activated the Togni I reagent and initiated a radical mechanism. This asymmetric three-component reaction between an enamine, Togni I reagent, and a nucleophile proceeded in the absence of a metal or photocatalyst. Of pertinence to the present work, the oxytrifluoromethylation reaction performed with water as the nucleophile afforded a single example of β-CF_3 alcohol in 59% yield and 80% ee.

In their investigation of the reductive asymmetric aza-Mislow-Evans rearrangement using 1,3,2-diazaphospholene hydrides (DAP-H), Cramer and coworkers described the enantioenriched synthesis of α-hydroxyamides (Scheme 34).[56] The Mislow-Evans rearrangement is a [2,3]-sigmatropic rearrangement, wherein an allylic sulfoxide is converted to a sulfenate ester *via* a five-membered transition state. This occurs with good diastereoselectivity, and the stereochemistry of the sulfur atom dictates the stereochemical outcome. Addition of a reductant can generate an allylic alcohol from the sulfenate ester. Typically, low temperatures and a strong base are required for this transformation. However, under the author's conditions, mild conditions at room temperature were achieved in the absence of a strong base by applying

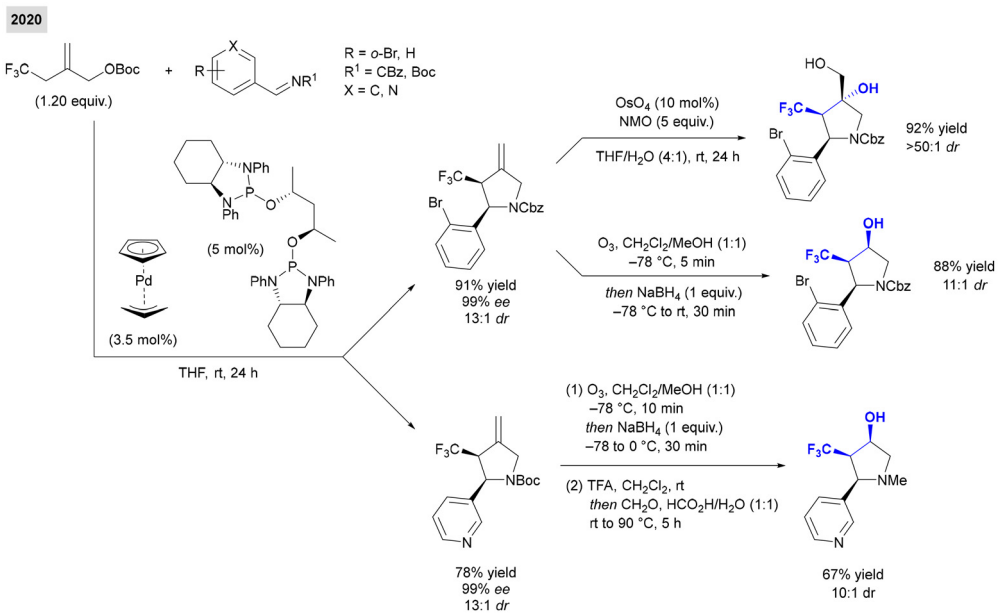

Scheme 32 Synthesis of trifluoromethyl pyrrolidines and subsequent transformations to generate β-CF_3 alcohols.

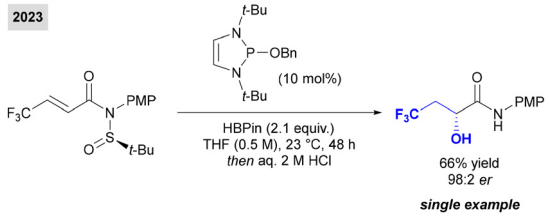

Scheme 34 Enantioenriched synthesis of α-hydroxyamide *via* Mislow–Evans rearrangement.

DAP-H as both the rearrangement catalyst and the reductant. In the scope, a single example of β-CF_3 alcohol was generated in 66% yield and 98 : 2 er, and required additional reaction time compared to electron-donating substrates in the scope.

3.2 Hydrogenation of alkenes

In their 2018 publication, Andersson and coworkers described the use of an azabicyclo iridium-oxazoline phosphine complex catalyst to accomplish the asymmetric hydrogenation of tetra-substituted vinyl fluorides (Scheme 35A).[57] As such, the authors reported the generation of two contiguous stereocenters in a single step, with one stereocenter bearing a fluorine atom. Four examples of β-F alcohols were demonstrated, without any defluorination side product formed for these substrates, in 74–99% yield, >99% dr, and 91–97% ee. A subsequent publication by Andersson and coworkers in 2020 focused on the asymmetric hydrogenation of an allylic alcohol motif to generate 1,2-fluorohydrins using a related azabicyclo thiazole-phosphine iridium complex (Scheme 35B).[58] The reaction was demonstrated on aromatic (*ortho*-, *para*-), heterocyclic (thiophenyl, naphthyl), and polyflyorinated substrates of varying substitution patterns. Aliphatic substrates were demonstrated (acyclic, cyclic, primary, secondary, tertiary). Notably, both *E*- and *Z*-isomers of 2-fluoro-4-phenylbut-2-en-1-ol were tested. The *E*-isomer resulted in 65% ee, 99% conversion (*S*)- and the *Z*-isomer gave 97% ee, 99% conversion for the opposite (*R*)-enantiomer, due to the steric control on facial selectivity. The reaction was demonstrated on gram scale, and further derivatization was shown towards a dapoxetine analogue. Allylic acetates were further demonstrated as viable substrates.

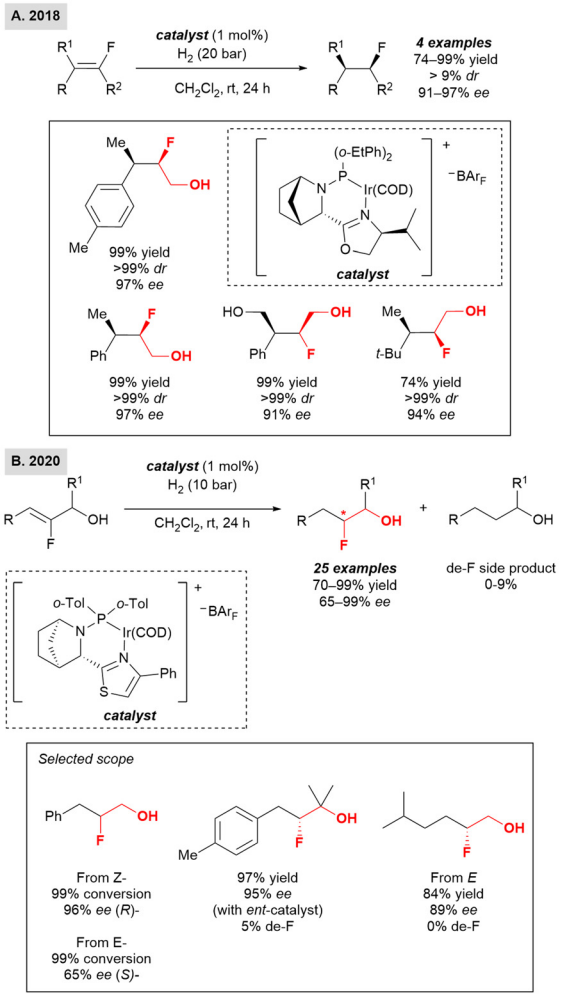

Scheme 35 Iridium catalyzed asymmetric hydrogenation of allylic alcohols.

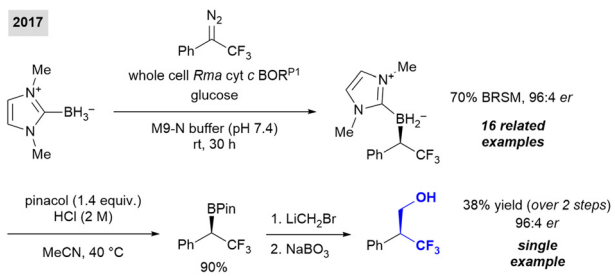

Scheme 36 Matteson homologation–oxidation of chiral organoboranes.

4 Reactions of organoboranes

With the assistance of *Escherichia coli* whole cells expressing a variant of cytochrome *c* from *Rhodothermus marinus*, Arnold and coworkers developed the synthesis of chiral organoboranes (Scheme 36).[59] The synthesis was performed up to gram scale, and 16 examples were given in enantiomeric ratio of 90 : 10 er to >99 : 1 er. Varying boron reagents and diazo ester substituents were tested in this scope, and it was determined that, since the steric bulk of the ester substituent did not affect the enzyme reactivity, this portion of the molecule was likely solvent exposed and not in the enzyme active site. The whole cell conditions outcompeted those using purified protein or cell lysate. The enantiopreference of the reaction was demonstrated to be tunable by further mutation of the enzyme, and was demonstrated on the illustrated example, which was afforded in 90 : 10 er for (*S*)- compared to 96 : 4 er (*R*)-. Derivatization of the products were demonstrated, includ-

ing a Matteson homologation-oxidation to afford the trifluoromethylated alcohol depicted.

Carreras and coworkers disclosed an enantioselective cyclopropanation reaction between trifluorodiazoethane and alkenyl boronates (Scheme 37).[60] Catalysed by a copper(I)-bisoxazoline complex, this reaction was demonstrated across 16 examples with yields in the neighbourhood of 40–77%, stereoselectivity of 89 : 11 to 97 : 3 er and diastereoselectivity of 86 : 14 to 95 : 5 dr. Further derivatization of a model substrate was performed, generating a fluorohydrin motif by hydrolysis of the boronate ester in 68% yield.

T. Xu and coworker reported the synthesis of various chiral perfluoroalkylated boronate esters through an enantioselective nickel-catalyzed reductive cross coupling (Scheme 38).[61] Perfluoroalkyl α-iodoboronates were readily accessed from perfluoroalkyl iodides and vinyl boronates, which in turn were reacted with aryl iodides. The authors determined that the chloride ion introduced by tetrabutylammonium chloride (TBAC) was essential to the outcome of the reaction, which proceeded through a radical mechanism. One example of trifluoromethyl product was generated, in 51% yield and 94 : 6 er.

Ge and coworkers described the hydroboration of fluorinated alkenes with pinacolborane (HBpin) under cobalt catalysis, in the presence of a biphosphine ligand (Scheme 39).[62] Thirty examples of enantioenriched CF_3-boranes were generated in 54–86% yield and 84–98% ee for aromatic and hetero-

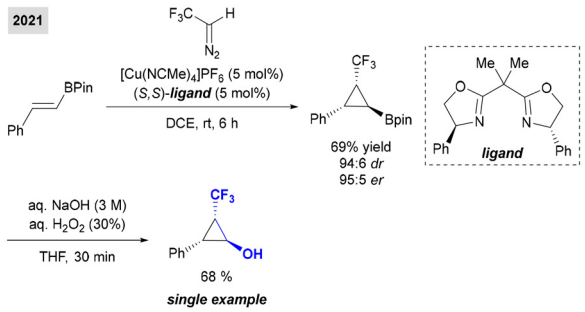

Scheme 37 Copper-catalysed enantioselective cyclopropanation and subsequent boronate ester hydrolysis.

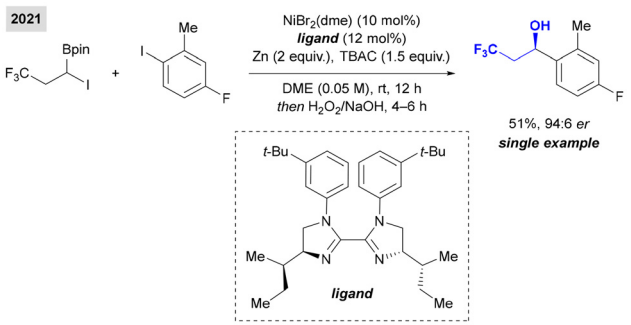

Scheme 38 Enantioselective nickel-catalyzed reductive cross coupling of perfluoroalkyl α-iodoboronates and aryl iodides.

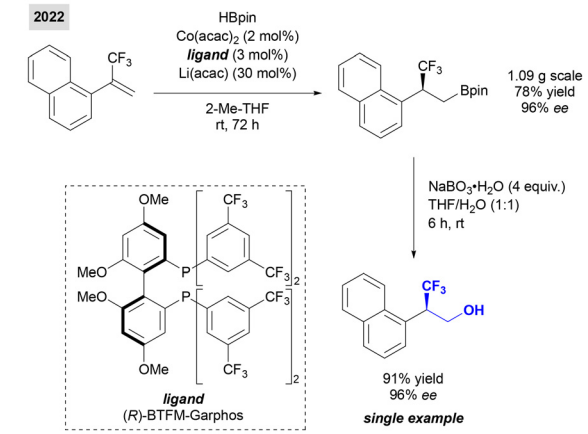

Scheme 39 Hydroboration of fluorinated alkenes with pinacolborane under cobalt catalysis.

aromatic substrates; one example of alkyl substrate was achieved in 78% yield, 52% ee. Pertinent here is the one example of further synthetic derivatization, where through oxidation the corresponding β-CF_3 alcohol was generated in 71% yield and 96% ee.

5 Cyclizations

5.1 Epoxide ring openings

G. Liu and coworkers described the palladium-catalysed oxidative trifluoromethoxylation of allylic C–H bonds (Scheme 40).[63] A scope of 26 aromatic compounds of varying complexity was demonstrated, affording yields ranging from 40–76%. An example of further derivatization was shown, where selective epoxidation of the title allylic compound (achieved in 76% yield by their method) selectively formed the (*E*)-isomer in 78% yield. Ring opening with an allylic Grignard reagent afforded the β-OCF_3 alcohol stereospecifically with 75% yield. On the one hand, the single example of alcohol demonstrates promise for this method to access β-OCF_3 alco-

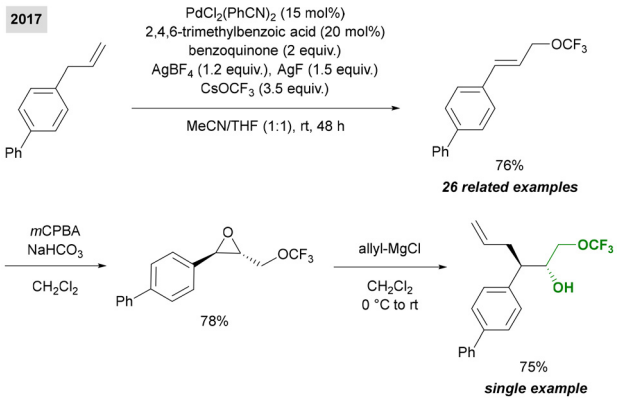

Scheme 40 Oxidative trifluoromethoxylation of allylic C–H bonds and further derivatization of one example to a β-OCF_3 alcohol.

hols, but the transformation conditions are still quite harsh and would result in side reactions for some substrates in the demonstrated reaction scope without further protection.

Tang and coworkers described in 2018 the trifluoromethoxylation of an epoxide to generate vicinal trifluoromethoxyhydrins (Scheme 41).[64] The reaction conditions invoked a cobalt catalyst with a salen ligand and nBu$_4$N$^+$DNP$^-$ to stabilize the -OCF$_3$, with trifluoromethyl arylsulfonate as the trifluoromethoxylation agent. This method was found robust for cyclic and acyclic substrates, but the enantioenrichment of scope molecules was not reported. The question of enantioselectivity was probed with a previously explored catalyst. Low levels of enantioenrichment (12% ee) were obtained for the desired compound, yet 87% ee was attained for the β-fluoro alcohol side product. This demonstrated that, during the epoxide ring opening transition state, the fluorinated product underwent a "head-to-tail" intramolecular bimetallic pathway. The trifluoromethoxylated product did not proceed by the same pathway, possibly due to steric repulsion between the CF$_3$ and either the epoxide or ligand, resulting in a loss in stereochemistry.

5.2 Ring expansion and cyclopropanation

Sun and coworkers described the asymmetric synthesis of 1,4-dioxanes and derivatives through chiral phosphoric acid catalysis, including one example of a β-CF$_3$ alcohol (Scheme 42).[65] This particular substrate had a slower reaction, likely due to decreased Lewis basicity of the oxetane substrate from trifluoromethyl electron withdrawal. Nearly zero conversion was observed at room temperature, such that the catalytic loading and temperature were increased to obtain the desired product in 92% yield and 98% ee.

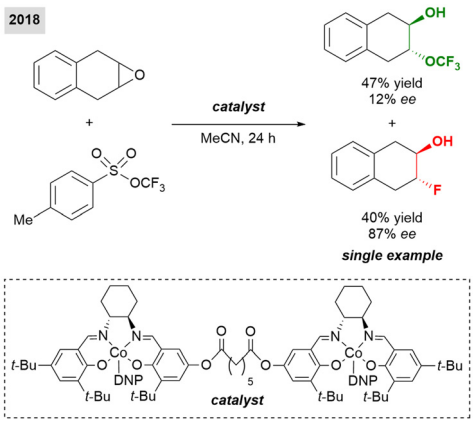

Scheme 41 Enantioselective example of trifluoromethoxylation of an epoxide by cobalt catalysis.

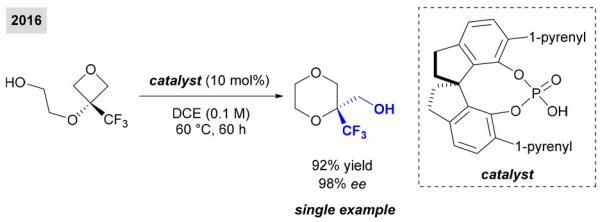

Scheme 42 Asymmetric synthesis of 1,4-dioxanes and derivatives through chiral phosphoric acid catalysis.

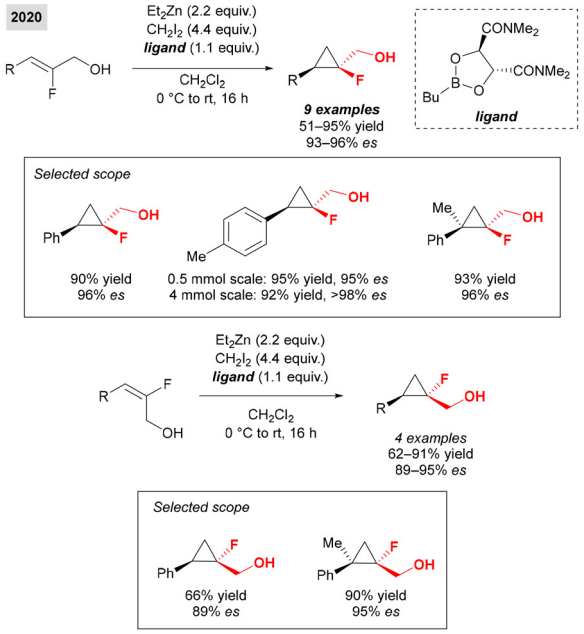

Scheme 43 Enantioselective cyclopropanation towards fluorinated cyclopropanes.

Charette and coworkers reported the enantioselective cyclopropanation with zinc carbenoids and chiral dioxaborolane ligand to generate fluorinated cyclopropanes (Scheme 43).[66] It was possible to tune the stereochemical outcome of the reaction by using either (*E*)- or (*Z*)- fluorinated allylic alcohols as the starting material of the reaction, with comparable enantioselectivity obtained in either case. The chiral diozaborolane ligand was able to stabilize the methylene transfer with the amide moieties, while complexing the allylic alkoxide substrate to the boron moiety. The reaction was scaled up to 4 mmol. For both (*E*)- and (*Z*)- alkenes, the generally observed trend indicated that electron rich substrates performed well, as did those with alkyl substitution or tetrasubstitution. However, reactivity was lower when an electron deficient group (halogen, CF$_3$) was present.

6 Selected applications in medicinal chemistry

6.1 Acyclic nucleosides

Herdewijn and coworkers unveiled a fluorohydrin motif during their enantioselective synthesis of 3-fluoro-2-(phosphonomethoxy)propyl acyclic nucleosides (FPMPs) (Scheme 44).[67] Acyclic nucleoside phosphonates are modified nucleosides which have demonstrated higher stability against hydrolysis than typical nucleosides, while still having the capacity to

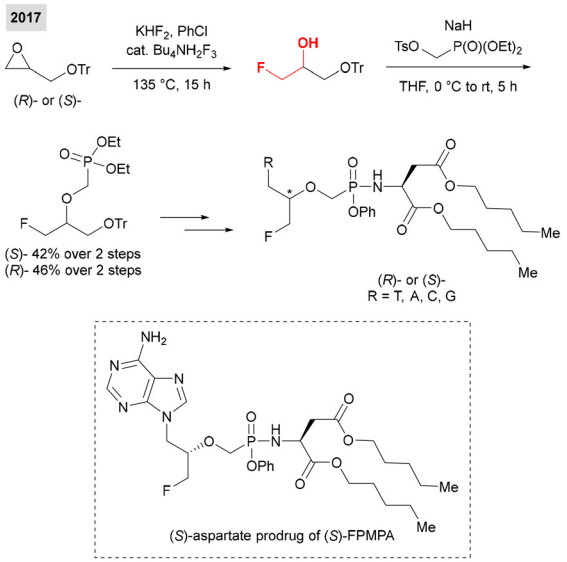

Scheme 44 Enantioselective synthesis of 3-fluoro-2-(phosphonomethoxy)propyl acyclic nucleosides (FPMPs).

undergo phosphorylation. When diphosphorylated (two phosphorylation steps), it is biologically analogous to nucleoside triphosphates (three phosphorylation steps). This is advantageous due to the typically rate limiting nature of the first phosphorylation step. Acyclic nucleoside phosphonates are flexible, which enables interaction with enzymes including DNA polymerase or reverse transcriptase. FPMPs are typically synthesized either through direct fluorination (which here afforded side products) or, as the authors opted, to incorporate a functionalized side chain. The ring opening of chiral O-tritylated glycidols resulted in the beta-F alcohol, which was further transformed into various FPMPs. One notable FPMP was the (S)-FPMPA amidate prodrug, which exhibited activity against HIV-1, hepatitis B virus (HBV), and varicella-zoster virus (VZV). It was stable in acidic and human plasma conditions but degraded with a half-life of 2 minutes in human liver microsome.

6.2 1-Lysoglycerophospholipid synthesis

Sano and coworkers generated a suite of 1-lysoglycerophospholipids (1-LPLs) analogues containing fluorine starting from the Still–Gennari reagent and Horner–Wadsworth–Emmons (HWE) reagent (Scheme 45).[68] LPLs function as signalling molecules in biological systems, and the equilibrium between 1-LPL (lysoglycerophospholipid with one acyl chain on the glycerol moiety) and 2-LPL (at the *sn*-1 position) governs the signaling pathways. Equilibrium is generally shifted towards 2-LPLs, but by replacing the hydroxyl with a fluorine atom, the acyl migration is blocked. Here, the authors transiently produced a halohydrin motif *en route* to a fluorinated analogue of 1-lysophosphatidylethanolamine (1-F-LPE). With a HWE reagent as a masked LPL and a chiral fluorinated alcohol, 1-F-LPE.HCl was generated in 16% over 7 steps, proceeding

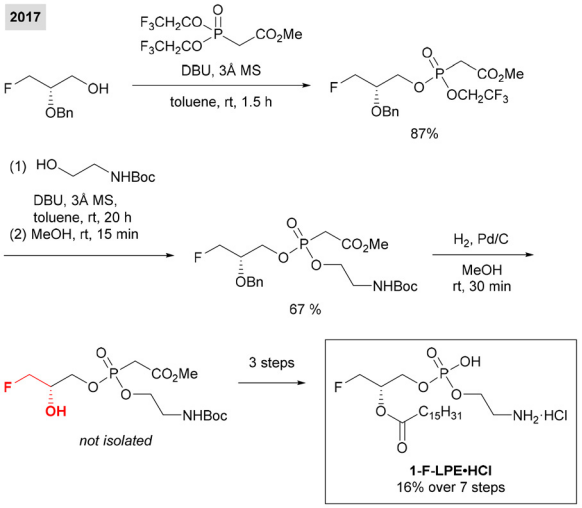

Scheme 45 Synthesis of 1-lysoglycerophospholipids (1-LPLs) analogues.

through a halohydrin motif that was unmasked in a hydrogenation step.

6.3 Covalent monoacylglycerol lipase inhibitor synthesis

McAllister and coworkers at Pfizer described their identification of PF-06795071 as a covalent monoacylglycerol lipase (MAGL) inhibitor upon optimization of the leaving group component (Scheme 46).[69] MAGL is a serine hydrolase responsible for the endocannabinoid pathway and arachidonoyl signaling

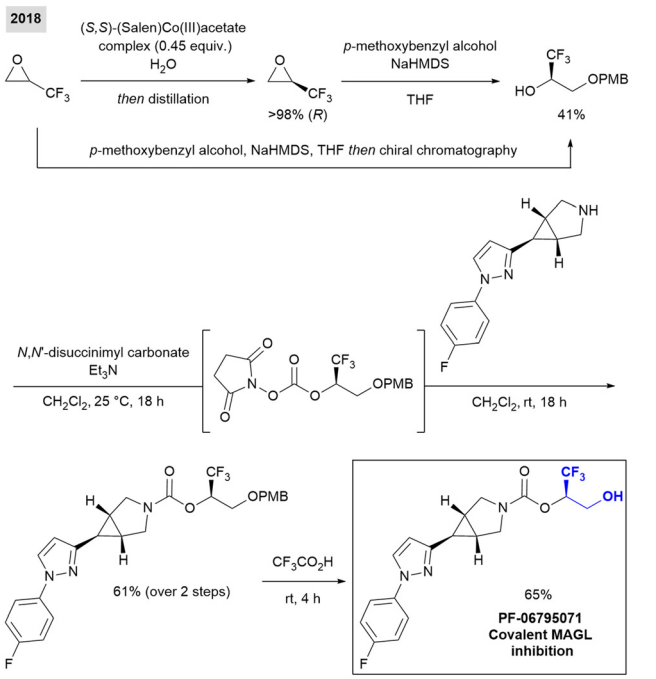

Scheme 46 Synthesis of a covalent monoacylglycerol lipase (MAGL) inhibitor.

in the central nervous system (CNS). It has been targeted to treat diseases involving neuroinflammation, such as Alzheimer's disease, Parkinson's disease, multiple sclerosis, pain, and acute brain injury. One key component of the target drug molecule was that it required a moiety that would both fit within the hydrophobic MAGL binding pocket. The drug also needed a component that could be hydrolysed and expulsed following the covalent inhibition modification event on the MAGL enzyme, similar to how the enzyme typically hydrolyses 2-arachidonyl glycerol and expulses glycerol. This group on the drug molecule was termed the "leaving group". While previous target iterations had employed a hexafluoroisopropanol (HFIP) leaving group, this was shown to be too lipophilic, with poor solubility and high clearance. As such, here a trifluoromethyl glycol leaving group was determined suitable, as it afforded excellent CNS permeability, as well as properties including solubility, selectivity, and low chemical reactivity. Once the motif and more potent enantiomer were identified, the trifluoromethyl glycol unit was introduced asymmetrically by either nucleophilic addition onto the racemic epoxide, the products of which can be separated on chiral chromatography, or by first performing kinetic resolution to obtain the desired epoxide, which avoids the chiral chromatography step. The protecting PMB group is cleaved as the final synthetic step to unveil the β-CF_3 alcohol motif.

6.4 Glucosylceramide synthase inhibitor synthesis

Loughran and their coworkers at Merck described their late-stage optimization towards an orally available Parkinson's disease (PD) therapy (Scheme 47).[70] One of the hallmarks of PD occurs due to mutations in the lysosomal enzyme glucocerebrosidase (GCase). This enzyme is supposed to metabolize the glycolipids glucosylceramide and glucosylsphingosine, but its mutation results in a buildup of these glycolipids and of misfolded protein α-synuclein. A treatment strategy is to decrease levels of glycolipids by introducing a glucosylceramide synthase (GCS) inhibitor. As such, the authors sought to develop a brain penetrant, orally bioavailable GCS inhibitor. In this report, the screening hit was improved by a difluorination of the isoindolinone core to increase drug potency. By replacing the cyclopropyl side chain with a trifluoromethyl group, there was a decline in potency, but the drug was less susceptible to recognition by P-gp. P-gp is a blood brain barrier efflux transporter; recognition by this transporter decreases the level of penetration of the drug to the brain. With respect to the synthesis of the compound of interest, the trifluoromethyl was introduced with ethyl 3,3,3-trifluoro-2-oxopropanoate. SFC and crystallization were performed as the final step of the racemic synthesis to afford the (*S*)-enantiomer, as determined by X-ray structure and vibrational circular dichroism (VCD).

6.5 Radiochemistry

Fluorine-18 is a commonly used radiolabeling isotope, notably due to its half-life of 109.8 min (compared to Carbon-11's half-life of 20.1 min).[71] The 3-[^{18}F]fluoro-2-hydroxypropyl ([^{18}F]FHP) group has shown utility in positron emission tomography (PET) imaging tracers, such as [^{18}F]fluoromisonidazole ([^{18}F]FMISO) for hypoxia imaging and [^{18}F]PM-PBB3 or [^{18}F]APN-1607 for tauopathy imaging (Fig. 3).[72] One of the two gold-standard biomarkers for Alzheimer's disease (AD) is the presence of intracellular neurofibrillary tangles (NFTs), which comprise of hyperphosphorylated Tau proteins.[73] The identification of these Tau protein tangles allows for the diagnosis of Alzheimer's disease, and the degree of misfold determines the

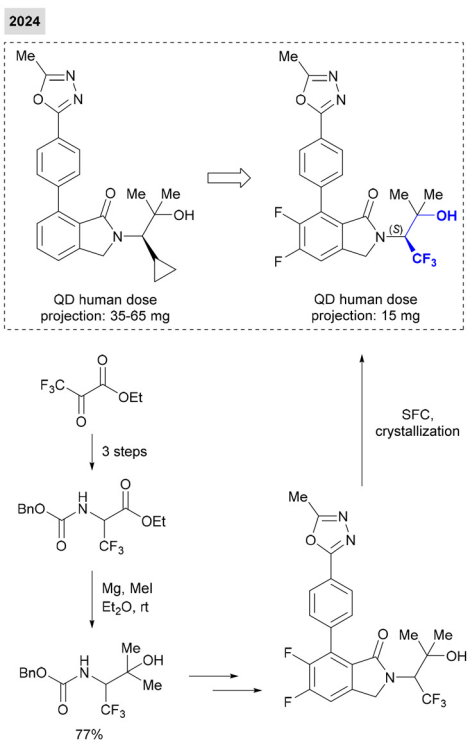

Scheme 47 Synthesis of a glucosylceramide synthase inhibitor.

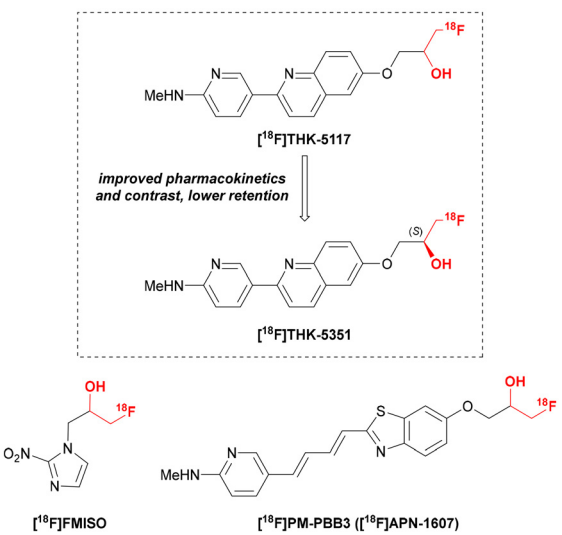

Fig. 3 [^{18}F] fluoro-2-hydroxypropyl ([^{18}F]-FHP)-containing PET tracers.

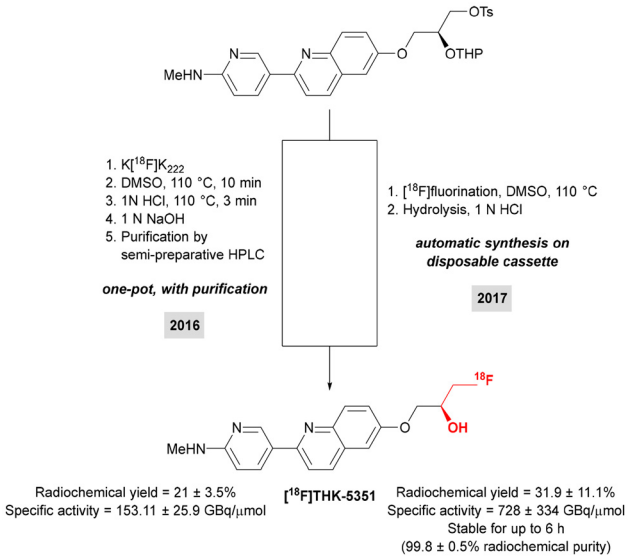

Scheme 48 Protocols for the preparation of [^{18}F]THK-5351.

disease state progression. While it is possible to measure the level of tangles in cerebrospinal fluid acquired through lumbar puncture, this does not provide information about the distribution of tangles in the brain, and it is an invasive procedure. As such, it is desirable to design PET probes to visualize and quantify tangles in the brain for non-invasive diagnosis of Alzheimer's disease. A first generation of PET Tau tracers have exhibited high selectivity and received FDA approval.[73] One tracer candidate, [^{18}F]THK-5351, is the single (*S*)-enantiomer of [^{18}F]THK-5117, and exhibits improved pharmacokinetics, contrast, and decreased retention relative to the racemic candidate (Fig. 3).[74]

In an effort to improve clinical drug supply, Yokell and coworkers reported a one pot, two step automated radiosynthesis of [^{18}F]THK-5351, followed by purification by semi-preparative HPLC and SPE cartridge reformulation with 10% ethanol in 0.9% sodium chloride (Scheme 48).[75] The uncorrected radiochemical yield was reported to be 21 ± 3.5%, with a specific activity of 153.11 ± 25.9 GBq μmol^{-1} and 96 ± 2% radiochemical purity after a 63 min synthesis with n = 3 experiments. Subsequently, Oh and coworkers developed a pH-controlled radiofluorination protocol within a fully automated, disposable, all-in-one cassette.[74] This method was shown to be reproducible and reliable throughout the 22 tests performed over a year and exhibited higher yield and less impurities than a previously described method. Production yield was reported to be 31.9 ± 11.1%, with a radiochemical purity of 99.8 ± 0.5%.

7 Conclusions

Fluorohydrins (β-F alcohols) and their fluorinated group (CF_3, OCF_3, and SCF_3) analogues have demonstrated a high degree of pertinence in bioactive compounds. Versatile methods have been demonstrated to afford access to multiple different fluorinated group analogues *via* a single set of reaction conditions. Complementary approaches to overcoming synthetic pitfalls, such as an unstable trifluoroethyl anion intermediate, have resulted in a myriad of new molecular motifs to explore. Recent advances in SF_5 chemistry have uncovered the racemic synthesis of β-SF_5 alcohols through the photochemical activation of SF_5Cl in the presence of oxygen,[76] however, the enantioselective synthesis of this motif remains to be seen. Further development of asymmetric routes towards newer group fluorohydrins, such as SF_5, or the underdeveloped NCF_3,[77] as well as the elaboration of enantioselective routes towards OCF_3 and SCF_3, would be interesting research targets in coming years.

Data availability

Data sharing is not applicable to this article as no datasets were generated or analyzed during the current study.

Conflicts of interest

There are no conflicts to declare.

Acknowledgements

We gratefully acknowledge the financial support of the Natural Sciences and Engineering Research Council of Canada, the Fonds de recherche – Nature et technologies and the Université Laval.

References

1 M. Inoue, Y. Sumii and N. Shibata, *ACS Omega*, 2020, **5**, 10633–10640.
2 N. A. Meanwell, *J. Med. Chem.*, 2018, **61**, 5822–5880.
3 P. Kirsch, *Modern Fluoroorganic Chemistry: Synthesis, Reactivity, Applications*, Wiley, 2nd edn, 2013, pp. 299–350.
4 A. L. Allred, *J. Inorg. Nucl. Chem.*, 1961, **17**, 215–221.
5 J. E. Huheey, *J. Phys. Chem.*, 1965, **69**, 3284–3291.
6 L. P. Hammett, *J. Chem. Soc.*, 1937, **59**, 96–103.
7 D. H. McDaniel and H. C. Brown, *J. Org. Chem.*, 1958, **23**, 420–427.
8 C. Hansch, A. Leo and R. W. Taft, *Chem. Rev.*, 1991, **91**, 165–195.
9 W. A. Sheppard, *J. Am. Chem. Soc.*, 1963, **85**, 1314–1318.
10 C. Hansch, A. Leo and R. W. Taft, *Chem. Rev.*, 1991, **91**, 165–195.
11 E. Sánchez-Díez, M. Fernández, U. Uria, E. Reyes, L. Carrillo and J. L. Vicario, *Chem. – Eur. J.*, 2015, **21**, 8384–8388.
12 H. Chachignon, E. V. Kondrashov and D. Cahard, *Adv. Synth. Catal.*, 2018, **360**, 965–971.

13 M. Y. Jin, J. Li, R. Huang, Y. Zhou, L. W. Chung and J. Wang, *Chem. Commun.*, 2018, **54**, 4581–4584.
14 S.-S. Li, S. Sun and J. Wang, *Angew. Chem., Int. Ed.*, 2022, **61**, e202115098.
15 B. B. Wu, J. Xu, K. J. Bian, Q. Gao and X.-S. Wang, *J. Am. Chem. Soc.*, 2022, **144**, 6543–6550.
16 D. Lin, Y. Chen, Z. Dong, P. Pei, H. Ji, L. Tai and L.-A. Chen, *CCS Chem.*, 2023, **5**, 1386–1397.
17 S. Wang, C. Zhang, D. Li, Y. Zhou, Z. Su, X. Feng and S. Dong, *Sci. China. Chem.*, 2023, **66**, 147–154.
18 Z. Xiong, F. Xu, Y. Zhou, R. Zhang, Y. Zhang, Y. Chen, W. Yao and Z. Wang, *Org. Lett.*, 2023, **25**, 8302–8307.
19 L. Bacheley, G. Guillamot, P. Phansavath and V. Ratovelomanana-Vidal, *Tetrahedron*, 2024, **152**, 133781.
20 X. Zhang, J. Qin, X. Huang and E. Meggers, *Eur. J. Org. Chem.*, 2018, 571–577.
21 A. S. Burns, C. C. Ross and S. D. Rychnovsky, *J. Org. Chem.*, 2018, **83**, 2504–2515.
22 K. Nicholson, J. Dunne, P. DaBell, A. B. Garcia, A. D. Bage, J. H. Docherty, T. A. Hunt, T. Langer and S. P. Thomas, *ACS Catal.*, 2021, **11**, 2034–2040.
23 T. Z. Zhu, P. L. Shao and X. Zhang, *Org. Chem. Front.*, 2021, **8**, 3705–3711.
24 A. E. Cotman, P. A. Dub, M. Sterle, M. Lozinšek, J. Dernovšek, Ž Zajec, A. Zega, T. Tomašič and D. Cahard, *ACS Org. Inorg. Au*, 2022, **2**, 396–404.
25 R. Molina Betancourt, P. Phansavath and V. Ratovelomanana-Vidal, *J. Org. Chem.*, 2021, **86**, 12054–12063.
26 R. Molina Betancourt, P. Phansavath and V. Ratovelomanana-Vidal, *Molecules*, 2022, **27**, 995.
27 R. Molina Betancourt, L. Bacheley, A. Karapetyan, G. Guillamot, P. Phansavath and V. Ratovelomanana-Vidal, *ChemCatChem*, 2022, **14**, e202200595.
28 L. Bacheley, R. Molina Betancourt, R. Ravindra, G. Guillamot, P. Phansavath and V. Ratovelomanana-Vidal, *Eur. J. Org. Chem.*, 2023, e202300383.
29 M. Sterle, M. Huš, M. Lozinšek, A. Zega and A. E. Cotman, *ACS Catal.*, 2023, **13**, 6242–6248.
30 P. R. Tharra, J. Švejkar, A. S. Jadhav, M. Nečas, P. A. Dub, M. D. Halls and J. Švenda, *J. Org. Chem.*, 2024, **89**, 12902–12911.
31 P. R. Tharra, A. A. Mikhaylov, J. Švejkar, M. Gysin, S. N. Hobbie and J. Švenda, *Angew. Chem., Int. Ed.*, 2022, **61**, e202116520.
32 D. Alsafadi, S. Alsalman and F. Paradisi, *Org. Biomol. Chem.*, 2017, **15**, 9169–9175.
33 M. M. Musa, *ChemistryOpen*, 2022, **11**, e202100251.
34 J. Fan, Y. Peng, W. Xu, A. Wang, J. Xu, H. Yu, X. Lin and Q. Wu, *Org. Lett.*, 2020, **22**, 5446–5450.
35 P. Ji, J. Park, Y. Gu, D. S. Clark and J. F. Hartwig, *Nat. Chem.*, 2021, **13**, 312–318.
36 T. Broese, P. Ehlers, P. Langer and J. von Langermann, *ChemBioChem*, 2021, **22**, 3314–3318.
37 Y. Zhang, H. Liu, Q. Shi, X. Chen and X. Xie, *Green Chem.*, 2022, **24**, 7889–7893.
38 A. Valotta, J. Maderbacher, T. Reiter, W. Kroutil and H. Gruber-Woelfler, *Chem. Pap.*, 2024, **78**, 7973–7986.
39 D. Cantillo, O. de Frutos, J. A. Rincón, C. Mateos and C. O. Kappe, *Org. Lett.*, 2014, **16**, 896–899.
40 M.-Y. Rong, L. Yang, J. Nie, F.-G. Zhang and J.-A. Ma, *Org. Lett.*, 2019, **21**, 4280–4283.
41 A. Matsuzawa, H. Noda, N. Kumagai and M. Shibasaki, *J. Org. Chem.*, 2017, **82**, 8304–8308.
42 K. Lee, D. L. Silverio, S. Torker, D. W. Robbins, F. Haeffner, F. W. van der Mei and A. H. Hoveyda, *Nat. Chem.*, 2016, **8**, 768–777.
43 F. W. van der Mei, C. Qin, R. J. Morrison and A. H. Hoveyda, *J. Am. Chem. Soc.*, 2017, **139**, 9053–9065.
44 D. C. Fager, K. Lee and A. H. Hoveyda, *J. Am. Chem. Soc.*, 2019, **141**, 16125–16138.
45 X. Fang, S. Wen, P. Jin, W. Bao, S. Liu, H. Cong and X. Shen, *ACS Catal.*, 2022, **12**, 2150–2157.
46 R. Hemelaere, J. Desroches and J.-F. Paquin, *Org. Lett.*, 2015, **17**, 1770–1773.
47 X. Liu, R. An, X. Zhang, J. Luo and X. Zhao, *Angew. Chem., Int. Ed.*, 2016, **55**, 5846–5850.
48 G. H. Schmid, *Phosphorus, Sulfur Relat. Elem.*, 1988, **36**, 197–200.
49 J. Xu, Y. Zhang, T. Qin and X. Zhao, *Org. Lett.*, 2018, **20**, 6384–6388.
50 M. Holmes, K. D. Nguyen, L. A. Schwartz, T. Luong and M. J. Krische, *J. Am. Chem. Soc.*, 2017, **139**, 8114–8117.
51 L. A. Schwartz, M. Holmes, G. A. Brito, T. P. Gonçalves, J. Richardson, J. C. Ruble, K. W. Huang and M. J. Krische, *J. Am. Chem. Soc.*, 2019, **141**, 2087–2096.
52 W.-S. Huang, M.-L. Delcourt, X. Pannecoucke, A. B. Charette, T. Poisson and P. Jubault, *Org. Lett.*, 2019, **21**, 7509–7513.
53 X. C. Gan and L. Yin, *Org. Lett.*, 2019, **21**, 931–936.
54 B. M. Trost, Y. Wang and C.-I. Hung, *Nat. Chem.*, 2020, **12**, 294–301.
55 H. Liang, D.-S. Ji, G.-Q. Xu, Y.-C. Luo, H. Zheng and P.-F. Xu, *Chem. Sci.*, 2022, **13**, 1088–1094.
56 G. Zhang and N. Cramer, *Angew. Chem., Int. Ed.*, 2023, **62**, e202301076.
57 S. Ponra, W. Rabten, J. Yang, H. Wu, S. Kerdphon and P. G. Andersson, *J. Am. Chem. Soc.*, 2018, **140**, 13878–13883.
58 S. Ponra, J. Yang, H. Wu, W. Rabten and P. G. Andersson, *Chem. Sci.*, 2020, **11**, 11189–11194.
59 S. B. J. Kan, X. Huang, Y. Gumulya, K. Chen and F. H. Arnold, *Nature*, 2017, **552**, 132–136.
60 J. Altarejos, D. Sucunza, J. J. Vaquero and J. Carreras, *Org. Lett.*, 2021, **23**, 6174–6178.
61 D. Wang and T. Xu, *ACS Catal.*, 2021, **11**, 12469–12475.
62 M. Hu, B. B. Tan and S. Ge, *J. Am. Chem. Soc.*, 2022, **144**, 15333–15338.
63 X. Qi, P. Chen and G. Liu, *Angew. Chem., Int. Ed.*, 2017, **56**, 9517–9521.
64 J. Liu, Y. Wei and P. Tang, *J. Am. Chem. Soc.*, 2018, **140**, 15194–15199.

65 W. Yang and J. Sun, *Angew. Chem., Int. Ed.*, 2016, **55**, 1868–1871.
66 L. Delion, T. Poisson, P. Jubault, X. Pannecoucke and A. B. Charette, *Can. J. Chem.*, 2020, **98**, 516–523.
67 M. Luo, E. Groaz, G. Andrei, R. Snoeck, R. Kalkeri, R. G. Ptak, T. Hartman, R. W. Buckheit, Jr., D. Schols, S. De Jonghe and P. Herdewijn, *J. Med. Chem.*, 2017, **60**, 6220–6238.
68 M. Nakao, K. Tanaka, S. Kitaike and S. Sano, *Synthesis*, 2017, 3654–3661.
69 L. A. McAllister, C. R. Butler, S. Mente, S. V. O'Neil, K. R. Fonseca, J. R. Piro, J. A. Cianfrogna, T. L. Foley, A. M. Gilbert, A. R. Harris, C. J. Helal, D. S. Johnson, J. I. Montgomery, D. M. Nason, S. Noell, J. Pandit, B. N. Rogers, T. A. Samad, C. L. Shaffer, R. G. da Silva, D. P. Uccello, D. Webb and M. A. Brodney, *J. Med. Chem.*, 2018, **61**, 3008–3026.
70 H. M. Loughran, K. M. Schirripa, A. J. Roecker, M. J. Breslin, L. Tong, K. L. Fillgrove, Y. Kuo, K. Bleasby, H. Collier, M. D. Altman, M. C. Ford, J. A. Newman, R. E. Drolet, M. Cosden, S. Jinn, R. B. Flick, X. Liu, C. Minnick, M. L. Watt, W. Lemaire, C. Burlein, G. C. Adam, L. A. Austin, J. N. Marcus, S. M. Smith and M. E. Fraley, *ACS Med. Chem. Lett.*, 2024, **15**, 123–131.
71 M. Fujinaga, T. Ohkubo, T. Yamasaki, Y. Zhang, W. Mori, M. Hanyu, K. Kumata, A. Hatori, L. Xie, N. Nengaki and M.-R. Zhang, *ChemMedChem*, 2018, **13**, 1723–1731.
72 M. Fujinaga, T. Ohkubo, T. Yamasaki, K. Kumata, N. Nengaki and M. R. Zhang, *Org. Lett.*, 2022, **24**, 4024–4028.
73 K. Zhou, F. Yang, Y. Li, Y. Chen, X. Zhang, J. Zhang, J. Wang, J. Dai, L. Cai and M. Cui, *Mol. Pharm.*, 2021, **18**, 1176–1195.
74 S. J. Lee, S. J. Oh, E. H. Cho, D. H. Kim, S. Furumoto, N. Okamura and J. S. Kim, *J. Radioanal. Nucl. Chem.*, 2017, **314**, 1587–1593.
75 R. Neelamegam, D. L. Yokell, P. A. Rice, S. Furumoto, Y. Kudo, N. Okamura and G. El Fakhri, *J. Labelled Compd. Radiopharm.*, 2017, **60**, 140–146.
76 Y. Jiang, X. Meng, J. Zhang, G. Wu, X. Lin and S. Guo, *Nat. Commun.*, 2024, **15**, 9705.
77 S. Schiesser, H. Chepliaka, J. Kollback, T. Quennesson, W. Czechtizky and R. J. Cox, *J. Med. Chem.*, 2020, **63**, 13076–13089.